

# Optimal Beamforming and Time Allocation for Partially Wireless Powered Sensor Networks with Downlink SWIPT

Shiqi Gong, Shaodan Ma, Chengwen Xing and Guanghua Yang

**Abstract**—Wireless powered sensor networks (WPSNs) have emerged as a key development towards the future self-sustainable Internet of Things (IoT) networks. To achieve a good balance between self-sustainability and reliability, partially WPSNs with a mixed power solution are desirable for practical applications. Specifically, most of the sensor nodes are wireless powered but the key sensor node adopts traditional wire/battery power for reliability. As a result, this paper mainly investigates optimal design for the partially WPSNs in which simultaneous wireless information and power transfer (SWIPT) is adopted in the downlink. Two scenarios with space division multiple access (SDMA) and time division multiple access (TDMA) in the uplink are considered. For both the SDMA-enabled and TDMA-enabled partially WPSNs, joint design of downlink beamforming, uplink beamforming and time allocation is investigated to maximize the uplink sum rate while guaranteeing the quality-of-service (i.e., satisfying the downlink rate constraint) at the key sensor node. After analyzing the feasibility of uplink sum rate maximization problems and the influence of the downlink rate constraint, semi-closed-form optimal solutions for both SDMA-enabled and TDMA-enabled WPSNs are proposed with guaranteed global optimality. Complexity analysis is also provided to justify the advantage of the proposed solutions in low complexity. The effectiveness and optimality of the proposed optimal solutions are finally demonstrated by simulations.

**Index Terms**—WPSN, SWIPT, SDMA-enabled, TDMA-enabled, uplink sum rate.

## I. INTRODUCTION

As a new paradigm in communications, internet of things (IoT) can provide intelligent control and smart solutions for various tasks in our lives by connecting a large variety of devices [1]–[3]. It has been gradually applied in various applications from smart homes, healthcare to structural and environmental monitoring, and disaster warning and so on [4]–[8]. Usually IoT networks involve a large number of sensor nodes to collect and exchange information with data center and can also be regarded as wireless sensor networks (WSNs). The success of IoT networks heavily relies on the reliability and sustainability of the sensor nodes. When a large number of sensors are deployed, power supply for the sensor nodes becomes a challenging issue to be solved. Currently, there are several available solutions to power up the sensors. The first one is to wire the sensor to a fixed power supply through cables. The installation is time consuming and location dependent, and the wire connection also limits the mobility of sensors. The second one is to power sensors by batteries. However, batteries usually have short lifetime and their maintenance and replacement are costly and difficult, especially when sensors

are deployed in harsh environment or remote locations. It is even impossible when the sensors are deployed inside the building structures or human bodies [4], [5]. The third one is to self-harvest energy from natural energy sources, such as solar and wind. But the amount of harvested energy is unstable and affected by uncontrollable nature factors. Lately, a new solution “wireless power transfer (WPT)” was proposed [6]–[8]. It leverages the fact that energy could be transferred wirelessly through radio frequency (RF) signals. Compared to other natural based energy harvesting, the RF oriented energy harvesting is generally ubiquitous, predictable and steady with low cost [9], [10]. As reported in [9], the energy harvesters operating at 915MHz and using Dipole antennas can collect about 3.7mW and 1uW of wireless power from RF signals at distances of 0.6m and 6m, respectively. Meanwhile, advanced antenna and transceiver designs for realizing high RF energy harvesting efficiency have also been reported [10]. With high feasibility and a wide range of applications in IoT, wireless powered sensor networks (WPSNs) have thus gained considerable research interest recently.

Generally in WPSNs, wireless powered sensors firstly harvest energy from the downlink RF signal transmitted by a power source or a hybrid access point (H-AP) which serves dually as a power source and a data center, and then utilize the harvested energy for uplink information transmission [13]–[15]. With multiple sensors, the uplink transmission can be supported following spatial division multiple access (SDMA) or time division multiple access (TDMA) schemes. To achieve various objectives, optimal designs for SDMA-enabled and TDMA-enabled WPSNs are necessary and have been investigated in the literature [15]–[21]. Specifically, for SDMA-enabled WPSNs, the optimal H-AP beamforming was proposed for maximizing the uplink sum rate and maximizing the minimum uplink rate among multiple wireless powered sensors, respectively in [15] and [16]. In [17], uplink sum throughput maximization under various cooperation protocols in SDMA-enabled cognitive WPSNs was studied. Moreover, fairness-based uplink throughput maximization was discussed for multiple-input-multiple-output (MIMO) WPSNs in [18]. With respect to the TDMA-enabled WPSNs, [19], [20] studied the optimal time allocation for multiple energy harvesters to maximize uplink sum throughput for single-input-single-output (SISO) WPSNs. When multiple-input-single-output (MISO) TDMA-enabled WPSNs were considered, joint beamforming design and time allocation for uplink sum throughput maximization were investigated in [21]. It was found that

the downlink energy beamforming design for the H-AP was similar to that in the SDMA-enabled WPSNs. For TDMA-enabled WPSNs with separate multiple-antenna power source and single-antenna data center, sum throughput maximization through optimal beamforming and time allocation was investigated in [7]. Optimal solutions were proposed for two different scenarios, i.e., the power source and the sensor nodes belong to the same or different service operator(s).

All the aforementioned optimal designs consider fully wireless powered sensor networks, in which all the sensor nodes are wireless powered and the downlink is dedicated for wireless power transfer only<sup>1</sup>. However in practice, mixed power solution may be adopted to achieve enhanced reliability in WSNs. Particularly, most of the sensor nodes are wireless powered, but the key sensor node is powered up by traditional battery/wire power for reliable communications. This network can be regarded as a partially wireless powered sensor network. In this partially WPSN, dual functions of RF signals in wireless information and power transfer can be exploited simultaneously in the downlink to further improve the spectral efficiency. In other words, the downlink RF signals can carry not only energy to wireless powered sensors but also information to the key sensor node with traditional power supply, which results in simultaneous wireless information and power transfer (SWIPT) in the downlink [11], [12]. This partially WPSN with downlink SWIPT can achieve efficient communications with a simple mixed power supply solution and thus is attractive for practical applications [23]. Nevertheless, optimal design for such WPSNs with downlink SWIPT is rarely investigated due to the difficulty in coupled downlink and uplink design as well as mixed power and information transfer. As far as we know, there is only one available optimal design for WPSNs with downlink SWIPT reported in [23]. It considered a SDMA-enabled WPSN with multiple users. Multiple downlink SWIPT phases were introduced to sequentially transmit information to one sensor while power up the others and equal time duration was assumed for all the downlink and uplink phases. Joint design of downlink beamforming and uplink power allocation were investigated to maximize the minimum downlink and uplink signal-to-interference-and-noise ratios (SINRs).

Here we take a step forward to investigate joint design of beamforming and time allocation for partially WPSNs with downlink SWIPT. To guarantee quality of service (QoS) at the key sensor node with traditional power supply, downlink rate constraint is taken into account and uplink sum rate maximization under such downlink rate constraint is mainly concerned. The implementation of the downlink SWIPT as well as the consideration of downlink rate constraint makes the optimal design challenging and also differentiates our design from the prior ones [15]–[21], [23]. Both SDMA and TDMA schemes are considered for the uplink transmission. Notice that extra time allocation in the uplink is involved in the TDMA-enabled WPSNs with downlink SWIPT and its optimal design hasn't been discussed before. The formulated uplink sum rate

maximization problems for both SDMA-enabled and TDMA-enabled partially WPSNs are originally non-convex with coupled optimization variables. But they can be reformulated as concave problems through certain transformation. After analyzing the feasibility of uplink sum rate maximization problems and the influence of the downlink rate constraint, semi-closed-form optimal solutions for both SDMA-enabled and TDMA-enabled WPSNs are proposed with guaranteed global optimality. Complexity analysis is also provided to justify the advantage of our proposed solutions in low complexity. The effectiveness and optimality of our proposed optimal solutions are finally demonstrated by simulations.

The rest of the paper is organized as follows. The partially WPSNs are introduced and the optimal design problems are formulated in Section II. Feasibility analysis and problem reformulation are given in Section III. Semi-closed-form optimal solutions for SDMA-enabled and TDMA-enabled WPSNs are derived and meaningful insights in the optimal solutions are pointed out in Section IV. Simulation results are presented in Section V and finally conclusions are drawn in Section VI.

**Notation:** Throughout this paper, bold-faced lowercase and uppercase letters stand for vectors and matrices, respectively. The symbols  $\mathbf{A}^T$ ,  $\mathbf{A}^*$ ,  $\mathbf{A}^H$ ,  $\mathbf{A}^{-1}$  and  $\text{Tr}(\mathbf{A})$  denote transpose, conjugate, Hermitian, inverse and trace of matrix  $\mathbf{A}$ , respectively. In addition,  $\text{vec}(\cdot)$  denotes the vector formed by stacking the columns of a matrix, while  $\text{diag}[\cdot]$  represents a diagonal matrix constructed from a vector.  $\mathbf{I}_d$  denotes a  $d$ -dimensional identity matrix. All eigenvalues and singular values in our work are arranged in a decreasing order. Finally,  $a \rightarrow b$  indicates  $a$  approaches  $b$  and  $(a)^+ = \max(a, 0)$ .

## II. SYSTEM MODEL AND PROBLEM FORMULATION

As shown in Fig. 1, we consider a partially WPSN with  $K$  wireless powered sensor nodes, also called energy harvesters (ERs),  $E_k, \forall k \in \mathcal{K}, \mathcal{K} = \{1, \dots, K\}$ , one battery/wire powered sensor node, also called information receiver (IR), and one hybrid access point (H-AP). The H-AP serves as not only power source to power up the sensor nodes ERs but also the data center to communicate with all sensor nodes. The H-AP and ERs are equipped with  $N_B$  and  $N_U$  antennas for effective wireless power transfer and harvesting, respectively, while the single-antenna IR is considered. This mixedly powered sensor network leverages wireless power transfer technique to solve for the challenging power supply problem for the majority of the sensor nodes, while adopts traditional battery/wire power only at the key sensor node to guarantee its communications. It can achieve efficient communications with simple power supply solution and has a wide range of practical applications.

In the partially WPSNs, two different phases are involved for power transfer and communications. In the first downlink phase, the H-AP transfers power to the ERs and sends information to the IR simultaneously. In other words, SWIPT is conducted in the downlink. Then in the second uplink phase, all the sensor nodes transmit sensing data to the H-AP. Since the ERs do not have a fixed power supply, their data transmissions are only powered by the harvested energy in the first downlink phase.

<sup>1</sup>If the H-AP has information to be transmitted to the sensor nodes, the information can be transmitted in another dedicated downlink phase.

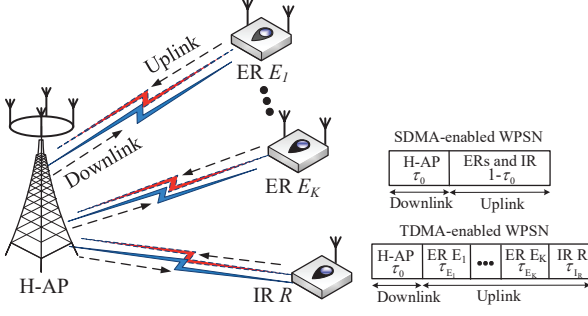


Fig. 1. SDMA-enabled and TDMA-enabled MIMO WPSNs.

Defining the total time duration for the two phases as a unit, we assume the first  $\tau_0$  ( $0 \leq \tau_0 \leq 1$ ) slot is utilized for downlink transmission and the remaining  $(1 - \tau_0)$  slot is allocated for uplink transmission. In the uplink transmission, two multiple access schemes, i.e., SDMA and TDMA, are considered. Specifically, for the SDMA-enabled WPSN, the IR and all ERs simultaneously transmit information to the H-AP in the  $(1 - \tau_0)$  slot, while for the TDMA-enabled WPSN, each ER and the IR sequentially transmit information to the H-AP in the  $\tau_{E_k}, \forall k \in \mathcal{K}$  and  $\tau_{I_R}$  slots, respectively, with  $\sum_{k=1}^K \tau_{E_k} + \tau_{I_R} = 1 - \tau_0$ . In general, SDMA outperforms TDMA in terms of uplink sum rate. However, TDMA is easy to implement with low signal detection complexity at the receiver. Both of them are widely adopted in wireless communication systems [21], [23].

#### A. SDMA-enabled WPSN

In the first downlink phase, the H-AP adopts the SWIPT technique to transmit energy and information to  $K$  ERs and the IR simultaneously. The energy-carrying information signal is denoted as  $\mathbf{s}_B \in \mathbb{C}^{N_B}$  with covariance matrix  $\mathbf{W}_B = \mathbb{E}[\mathbf{s}_B \mathbf{s}_B^H] \in \mathbb{C}^{N_B \times N_B}$ . The transmission power can be written as  $\text{tr}(\mathbf{W}_B)$  and should usually satisfy the power constraint  $\text{tr}(\mathbf{W}_B) \leq P_B$ , where  $P_B$  is the maximum allowable transmission power. Denoting the downlink channels from the H-AP to the IR and ER  $E_k$  as  $\mathbf{h}_{I_R} \in \mathbb{C}^{N_B}$  and  $\mathbf{H}_{E_k} \in \mathbb{C}^{N_U \times N_B}, \forall k \in \mathcal{K}$ , respectively, the received signals at  $K$  ERs and IR can be respectively written as

$$\mathbf{y}_{E_k} = \mathbf{H}_{E_k} \mathbf{s}_B + \mathbf{n}_{E_k}, \forall k \in \mathcal{K} \quad (1)$$

$$\mathbf{y}_{I_R} = \mathbf{h}_{I_R}^H \mathbf{s}_B + n_{I_R} \quad (2)$$

where  $\mathbf{n}_{E_k} \sim \mathcal{CN}(\mathbf{0}, \sigma_n^2 \mathbf{I}_{N_U})$  and  $n_{I_R} \sim \mathcal{CN}(0, \sigma_n^2)$  are the additive white Gaussian noises (AWGNs) at the ER  $E_k, \forall k \in \mathcal{K}$  and IR, respectively. According to (1), the harvested energy at ER  $E_k$  in this  $\tau_0$  slot can be expressed as

$$Q_{E_k} = \tau_0 \varepsilon_k \text{tr}(\mathbf{H}_{E_k} \mathbf{W}_B \mathbf{H}_{E_k}^H), \forall k \in \mathcal{K} \quad (3)$$

where  $0 \leq \varepsilon_k \leq 1$  denotes the energy harvesting efficiency of ER  $E_k, \forall k \in \mathcal{K}$ . Meanwhile, based on (2), the achievable downlink rate of the IR is expressed as

$$R_{I_R}^D = \tau_0 \log(1 + \sigma_n^{-2} \mathbf{h}_{I_R}^H \mathbf{W}_B \mathbf{h}_{I_R}). \quad (4)$$

In the second uplink stage, the IR and ER  $E_k$  simultaneously transmit the information signals  $\mathbf{s}_R$  with  $\mathbb{E}[|\mathbf{s}_R|^2] = 1$  and  $\mathbf{x}_{E_k} \in \mathbb{C}^{N_U}$  with covariance matrix  $\mathbf{P}_{E_k} = \mathbb{E}[\mathbf{x}_{E_k} \mathbf{x}_{E_k}^H] \in \mathbb{C}^{N_U \times N_U}$  to the H-AP, respectively. The transmission power at the IR is fixed as  $P_I$ . Since the energy at the ER  $E_k$  is only coming from energy harvesting in the first phase, the transmission energy at the ER  $E_k$  should not exceed the harvested energy  $Q_{E_k}$ , i.e.,  $(1 - \tau_0) \text{tr}(\mathbf{P}_{E_k}) \leq \tau_0 \varepsilon_k \text{tr}(\mathbf{H}_{E_k} \mathbf{W}_B \mathbf{H}_{E_k}^H), \forall k \in \mathcal{K}$ . By denoting  $\mathbf{g}_{I_R} \in \mathbb{C}^{N_B}$  and  $\mathbf{G}_{E_k} \in \mathbb{C}^{N_B \times N_U}$  as the uplink channels from the IR and ER  $E_k, \forall k \in \mathcal{K}$  to the H-AP, respectively, we have the received signal at the H-AP as

$$\mathbf{y}_B = \sum_{k=1}^K \mathbf{G}_{E_k} \mathbf{x}_{E_k} + \mathbf{g}_{I_R} \sqrt{P_I} \mathbf{s}_R + \mathbf{n}_B, \quad (5)$$

where  $\mathbf{n}_B \sim \mathcal{CN}(\mathbf{0}, \sigma_n^2 \mathbf{I}_{N_B})$  denotes the received AWGN noise at the H-AP. Similarly to [24], we assume that successive interference cancellation technique is adopted at the H-AP, and thus the achievable uplink sum rate of the SDMA-enabled WPSN can be formulated as

$$R_S^U = (1 - \tau_0) \log \det \left( \tilde{\mathbf{I}}_R + \sigma_n^{-2} \sum_{k=1}^K \mathbf{G}_{E_k} \mathbf{P}_{E_k} \mathbf{G}_{E_k}^H \right) \quad (6)$$

where  $\tilde{\mathbf{I}}_R = \mathbf{I}_{N_B} + \sigma_n^{-2} P_I \mathbf{g}_{I_R} \mathbf{g}_{I_R}^H$ . In this paper, we aim at maximizing the uplink sum rate  $R_S^U$  in (6) while guaranteeing the downlink communication quality-of-service (QoS), i.e., the downlink information rate  $R_{I_R}^D$  in (4), by jointly optimizing the time splitting ratio  $\tau_0$ , downlink energy beamforming  $\mathbf{W}_B$  and uplink information beamforming  $\mathbf{P}_{E_k}, \forall k \in \mathcal{K}$ . Mathematically, the uplink sum rate maximization problem in the SDMA-enabled WPSN is formulated as

$$\begin{aligned} \max_{\tau_0, \mathbf{W}_B \succeq \mathbf{0}, \mathbf{P}_{E_k} \succeq \mathbf{0}, \forall k} & (1 - \tau_0) \log \det \left( \tilde{\mathbf{I}}_R + \sigma_n^{-2} \sum_{k=1}^K \mathbf{G}_{E_k} \mathbf{P}_{E_k} \mathbf{G}_{E_k}^H \right) \\ \text{s.t. CR1:} & \text{tr}(\mathbf{W}_B) \leq P_B, \quad 0 \leq \tau_0 \leq 1, \\ \text{CR2:} & \tau_0 \log(1 + \sigma_n^{-2} \mathbf{h}_{I_R}^H \mathbf{W}_B \mathbf{h}_{I_R}) \geq R_I, \\ \text{CR3:} & (1 - \tau_0) \text{tr}(\mathbf{P}_{E_k}) \leq \tau_0 \varepsilon_k \text{tr}(\mathbf{H}_{E_k} \mathbf{W}_B \mathbf{H}_{E_k}^H), \forall k. \end{aligned} \quad (7)$$

Here, the constraint CR1 corresponds to the maximum transmission power constraint at the H-AP, CR2 models the downlink QoS constraint at the IR node where  $R_I$  denotes the required minimum downlink rate, and CR3 considers the uplink transmission energy constraints at the ERs since their uplink energies are only coming from the harvested energies  $Q_{E_k}$  (3) in the downlink. Notice that our uplink sum rate maximization is different from those for fully WPSNs in [15]–[21], since both energy and information transfers are conducted simultaneously in the downlink and additional downlink rate constraint CR2 is considered to guarantee the QoS for the information transfer to the IR. Moreover, our rate maximization problem also differs from that in [23] with additional uplink energy constraints CR3. Clearly, the downlink rate constraint and the uplink energy constraints are practical and necessary to be considered in partially WPSNs. However, their consideration complicates the optimization problem with highly coupled variables  $\{\tau_0, \mathbf{W}_B, \mathbf{P}_{E_k}, \forall k \in \mathcal{K}\}$ , and the problem becomes non-convex and difficult to solve.

### B. TDMA-enabled WPSN

For the TDMA-enabled WPSN, the received signals at the ER  $E_k$  and the IR in the downlink phase are the same as that in (1) and (2), respectively. However, in the uplink phase, the IR and each ER  $E_k$  sequentially transmit signals to the H-AP within the slots of  $\tau_{I_R}$  and  $\tau_{E_k}$ , respectively. Therefore, the achievable uplink sum rate is given by

$$R_T^U = \sum_{k=1}^K \tau_{E_k} \log \det(\mathbf{I}_{N_B} + \sigma_n^{-2} \mathbf{G}_{E_k} \mathbf{P}_{E_k} \mathbf{G}_{E_k}^H) + \tau_{I_R} \log(1 + \sigma_n^{-2} P_I \mathbf{g}_{I_R} \mathbf{g}_{I_R}^H) \quad (8)$$

Accordingly, the uplink sum rate maximization problem in the TDMA-enabled WPSN is formulated as

$$\begin{aligned} \max_{\boldsymbol{\tau}, \mathbf{W}_B \succeq \mathbf{0}, \mathbf{P}_{E_k} \succeq \mathbf{0}} \quad & \sum_{k=1}^K \tau_{E_k} \log \det(\mathbf{I}_{N_B} + \sigma_n^{-2} \mathbf{G}_{E_k} \mathbf{P}_{E_k} \mathbf{G}_{E_k}^H) \\ & + \tau_{I_R} \log \det(1 + \sigma_n^{-2} P_I \mathbf{g}_{I_R} \mathbf{g}_{I_R}^H) \\ \text{s.t. CR1: } & \text{tr}(\mathbf{W}_B) \leq P_B, \quad 0 \leq \tau_0 \leq 1, \\ \text{CR2: } & \tau_0 \log(1 + \sigma_n^{-2} \mathbf{h}_{I_R}^H \mathbf{W}_B \mathbf{h}_{I_R}) \geq R_I, \\ \text{CR4: } & \tau_{E_k} \text{tr}(\mathbf{P}_{E_k}) \leq \tau_0 \varepsilon_k \text{tr}(\mathbf{H}_{E_k} \mathbf{W}_B \mathbf{H}_{E_k}^H), \forall k, \\ \text{CR5: } & \tau_{I_R} + \sum_{k=1}^K \tau_{E_k} = 1 - \tau_0 \end{aligned} \quad (9)$$

where  $\boldsymbol{\tau} = [\tau_0, \tau_{E_1}, \dots, \tau_{E_K}, \tau_{I_R}]$ . Similarly to CR3 in (7), the constraint CR4 models the uplink transmission energy constraints but with the uplink slot for the ER  $E_k$  adjusted as  $\tau_{E_k}$ . Additionally, the constraint CR5 is introduced due to the implementation of TDMA protocol. Clearly, the problem (9) is also nonconvex and is more challenging than the problem (7) since more time slots are involved in the vector  $\boldsymbol{\tau}$  for optimization. Obviously, the key challenge in the problems (7) and (9) comes from the downlink rate constraint CR2, its feasibility will be discussed first before we proceed to solve for the optimization problems.

### III. FEASIBILITY ANALYSIS

#### A. Feasibility of downlink rate constraint

Different from most of the prior designs for WPSNs, downlink rate constraint CR2 is considered here due to the adoption of simultaneous wireless power and information transfer in the downlink. Clearly from (7) and (9), the feasible downlink rate threshold  $R_I$  is limited by the achievable downlink rate  $R_{I_R}^D$  in (4) which depends on the downlink beamforming  $\mathbf{W}_B$ , while  $\mathbf{W}_B$  is also constrained by the maximum downlink transmission power in CR1. The feasible downlink rate threshold is thus upper bounded by

$$\begin{aligned} \max_{\tau_0, \mathbf{W}_B \succeq \mathbf{0}} \quad & R_I \\ \text{s.t. CR1: } & \text{tr}(\mathbf{W}_B) \leq P_B, \quad 0 \leq \tau_0 \leq 1, \\ \text{CR2: } & \tau_0 \log(1 + \sigma_n^{-2} \mathbf{h}_{I_R}^H \mathbf{W}_B \mathbf{h}_{I_R}) \geq R_I. \end{aligned} \quad (10)$$

It is easily observed that the optimal  $\tau_0$  for the problem (10) is  $\tau_0 = 1$ , and then the problem (10) reduces to a conventional rate maximization problem for a MISO system and has been solved in [25]. More specifically, the optimal solution

of  $\mathbf{W}_B$  for the problem (10) is  $\mathbf{W}_B^{up} = \frac{P_B}{\|\mathbf{h}_{I_R}\|^2} \mathbf{h}_{I_R} \mathbf{h}_{I_R}^H$ , which means that the downlink beamforming is aligned for information transmission only. The upper bound of feasible downlink rate threshold is correspondingly given as  $R_I^{up} = \log(1 + \sigma_n^{-2} P_B \|\mathbf{h}_{I_R}\|^2)$  [25]. Since both SDMA-enabled and TDMA-enabled WPSNs have the same downlink process, this upper bound  $R_I^{up}$  is applicable for both problems (7) and (9). In other words, we can conclude that when  $R_I \in [0, R_I^{up}]$ , the problems (7) and (9) are feasible.

#### B. Tightness of downlink rate constraint

In the feasible region  $R_I \in [0, R_I^{up}]$ , the tightness of downlink rate constraint CR2 depends on the actual rate threshold  $R_I$  and will heavily affect the optimal solutions for the problems (7) and (9). Now we take the problem (7) for tightness investigation first. Specifically, if neglecting the downlink rate constraint CR2, the problem (7) reduces to the sum rate maximization problem for fully WPSNs in [17], and the corresponding optimal downlink beamforming is given as  $\mathbf{W}_B^{mi} = P_B \mathbf{u}_B^{mi} (\mathbf{u}_B^{mi})^H$ , where  $\mathbf{u}_B^{mi} \in \mathbb{C}^{N_B}$  is the dominated eigenvector of a certain linear combination of the covariance matrices for all ERs' downlink channels, i.e.,  $\mathbf{H}_{E_k} \mathbf{H}_{E_k}^H, \forall k \in \mathcal{K}$  [17]. This solution means that the downlink beamforming is aligned for energy transfer only.

Given this downlink beamforming, the achievable downlink rate can be expressed as  $R_I^{mi} = \log(1 + \sigma_n^{-2} \mathbf{h}_{I_R}^H \mathbf{W}_B^{mi} \mathbf{h}_{I_R})$ , and the corresponding optimal achievable uplink sum rate is in fact an upper bound of that of the problem (7) with the constraint CR2. If the downlink rate threshold  $R_I$  is less than the rate  $R_I^{mi}$ , i.e.,  $R_I < R_I^{mi}$ , the downlink rate constraint CR2 can be automatically satisfied with the inequality strictly holding, i.e.,  $\tau_0 \log(1 + \sigma_n^{-2} \mathbf{h}_{I_R}^H \mathbf{W}_B \mathbf{h}_{I_R}) > R_I$ . In other words, when  $R_I \in [0, R_I^{mi}]$ , the constraint CR2 is inactive and can be ignored in the problem (7). However, when  $R_I^{mi} \leq R_I \leq R_I^{up}$ , the downlink rate constraint cannot be ignored and we have the following result.

**Lemma 1.** *When  $R_I^{mi} \leq R_I \leq R_I^{up}$ , the downlink rate constraint in the problem (7) is tight, i.e., the optimal solution will exist at the boundary with  $\tau_0 \log(1 + \sigma_n^{-2} \mathbf{h}_{I_R}^H \mathbf{W}_B \mathbf{h}_{I_R}) = R_I$  satisfied.*

*Proof.* Please see Appendix A.  $\square$

With respect to the problem (9), by neglecting the constraint CR2, although the corresponding optimal downlink beamforming and the achievable downlink rate ( $\mathbf{W}_B^{mi}$  and  $R_I^{mi}$ ) cannot be directly obtained based on the results in [17] due to the extra time allocations  $\tau_{I_R}$  and  $\tau_{E_k}$ , they can be derived using the joint concavity of the problem (9) proved in Section III. C. Then the above tightness result also holds for the problem (9) in the TDMA-enabled WPSNs. Since the tightness proof is similar to that in Appendix A, it is omitted here for conciseness.

#### C. Problem reformulation

In order to solve the uplink sum rate maximization problem (7) for the SDMA-enabled WPSNs effectively, we define two

new variables  $\widetilde{\mathbf{W}}_B = \tau_0 \mathbf{W}_B$  and  $\widetilde{\mathbf{P}}_{E_k} = (1-\tau_0) \mathbf{P}_{E_k}, \forall k \in \mathcal{K}$ . Then the problem (7) can be reformulated as

$$\begin{aligned} \max_{\tau_0, \{\widetilde{\mathbf{W}}_B, \widetilde{\mathbf{P}}_{E_k}\} \succeq \mathbf{0}} & (1-\tau_0) \log \det \left( \widetilde{\mathbf{I}}_R + \frac{\sigma_n^{-2}}{1-\tau_0} \sum_{k=1}^K \mathbf{G}_{E_k} \widetilde{\mathbf{P}}_{E_k} \mathbf{G}_{E_k}^H \right) \\ \text{s.t. } \widetilde{\text{CR1}} : & \text{tr}(\widetilde{\mathbf{W}}_B) \leq P_B \tau_0, \quad 0 \leq \tau_0 \leq 1, \\ & \widetilde{\text{CR2}} : \tau_0 \log(1 + \frac{\sigma_n^{-2}}{\tau_0} \mathbf{h}_{I_R}^H \widetilde{\mathbf{W}}_B \mathbf{h}_{I_R}) \geq R_I \\ & \widetilde{\text{CR3}} : \text{tr}(\widetilde{\mathbf{P}}_{E_k}) \leq \varepsilon_k \text{tr}(\mathbf{H}_{E_k} \widetilde{\mathbf{W}}_B \mathbf{H}_{E_k}^H), \quad \forall k. \end{aligned} \quad (11)$$

Clearly, the objective function of the problem (11) is the perspective of the concave function  $f(\mathbf{P}_{E_k}) = \log \det(\widetilde{\mathbf{I}}_R + \sigma_n^{-2} \sum_{k=1}^K \mathbf{G}_{E_k} \mathbf{P}_{E_k} \mathbf{G}_{E_k}^H)$ . According to [26, p. 39], the concavity is preserved by the perspective operation. Therefore, the objective function is strictly and jointly concave with respect to (w.r.t.)  $\{\tau_0, \widetilde{\mathbf{P}}_{E_k}, \forall k \in \mathcal{K}\}$ . In addition, all constraints in (11) are convex. We then can conclude that the problem (11) is jointly concave w.r.t.  $\{\tau_0, \widetilde{\mathbf{W}}_B, \widetilde{\mathbf{P}}_{E_k}, \forall k \in \mathcal{K}\}$ . Similarly, by redefining  $\widetilde{\mathbf{P}}_{E_k} = \tau_{E_k} \mathbf{P}_{E_k}, \forall k \in \mathcal{K}$ , the uplink sum rate maximization problem (9) for TDMA-enabled WPSNs can also be reformulated as

$$\begin{aligned} \max_{\tau, \widetilde{\mathbf{W}}_B \succeq \mathbf{0}, \widetilde{\mathbf{P}}_{E_k} \succeq \mathbf{0}} & \sum_{k=1}^K \tau_{E_k} \log \det(\mathbf{I}_{N_B} + \frac{\sigma_n^{-2}}{\tau_{E_k}} \mathbf{G}_{E_k} \widetilde{\mathbf{P}}_{E_k} \mathbf{G}_{E_k}^H) \\ & + \tau_{I_R} \log \det(\mathbf{I}_{N_B} + \sigma_n^{-2} P_{I_R} \mathbf{g}_{I_R} \mathbf{g}_{I_R}^H) \\ \text{s.t. } & \widetilde{\text{CR1}}, \widetilde{\text{CR2}}, \widetilde{\text{CR3}}, \text{CR5}. \end{aligned} \quad (12)$$

Following a similar logic of proving the concavity of the problem (11), the problem (12) is also jointly concave w.r.t.  $\{\tau, \widetilde{\mathbf{W}}_B, \widetilde{\mathbf{P}}_{E_k}, \forall k \in \mathcal{K}\}$ . Both problems (11) and (12) can be numerically solved by standard convex optimization technique [26], and the globally optimal beamforming  $\mathbf{W}_B$  and  $\mathbf{P}_{E_k}$  and the time slots can then be obtained with simple variable substitution. However, the numerical solution not only has high computational complexity but also provides little insight. In the following, we will propose insightful semi-closed-form optimal solutions for the jointly concave problems with low complexity.

#### IV. SEMI-CLOSED-FORM OPTIMAL SOLUTIONS FOR SDMA-ENABLED AND TDMA-ENABLED WPSNS

It is noticed that when the time splitting ratio  $\tau_0$  is given, the problems (11) and (12) are still jointly concave w.r.t. the other design variables  $\{\widetilde{\mathbf{W}}_B, \widetilde{\mathbf{P}}_{E_k}, \forall k \in \mathcal{K}\}$ . It inspires us to solve for the optimal solution for the other design variables by fixing  $\tau_0$ , and then find the optimal  $\tau_0$  afterwards.

##### A. SDMA-enabled uplink sum rate maximization

When  $\tau_0$  is given, the SDMA-enabled uplink sum rate maximization problem (11) can be rewritten as

$$\begin{aligned} f_S(\tau_0) = \max_{\substack{\widetilde{\mathbf{W}}_B \succeq \mathbf{0}, \\ \widetilde{\mathbf{P}}_{E_k} \succeq \mathbf{0}, \forall k}} & (1-\tau_0) \log \det \left( \widetilde{\mathbf{I}}_R + \frac{\sigma_n^{-2}}{(1-\tau_0)} \sum_{k=1}^K \mathbf{G}_{E_k} \widetilde{\mathbf{P}}_{E_k} \mathbf{G}_{E_k}^H \right) \\ \text{s.t. } & \widetilde{\text{CR1}}, \widetilde{\text{CR2}}, \widetilde{\text{CR3}}, \end{aligned} \quad (13)$$

and its corresponding Lagrangian function is given by

$$\begin{aligned} L_S(\mathcal{A}_S) = & (1-\tau_0) \log \det \left( \mathbf{M}_{\mathcal{K} \setminus k}^{-1} + \frac{\sigma_n^{-2}}{(1-\tau_0)} \mathbf{G}_{E_k} \widetilde{\mathbf{P}}_{E_k} \mathbf{G}_{E_k}^H \right) \\ & + \text{tr} \left( (\widetilde{\mathbf{H}} + \mathbf{Z}_0) \widetilde{\mathbf{W}}_B \right) - \sum_{k=1}^K \text{tr}((\mu_k \mathbf{I}_{N_U} - \mathbf{Z}_k) \widetilde{\mathbf{P}}_{E_k}) + \epsilon_S, \end{aligned} \quad (14)$$

where  $\mathcal{A}_S = \{\widetilde{\mathbf{W}}_B, \widetilde{\mathbf{P}}_{E_k}, \mathbf{Z}_0, \lambda, \beta, \mathbf{Z}_k, \mu_k, \forall k\}$  and

$$\begin{aligned} \mathbf{M}_{\mathcal{K} \setminus k} &= \mathbf{M}_{\mathcal{K} \setminus k}^{\frac{1}{2}} \mathbf{M}_{\mathcal{K} \setminus k}^{\frac{1}{2}} = \left( \widetilde{\mathbf{I}}_R + \frac{\sigma_n^{-2}}{(1-\tau_0)} \sum_{i \neq k} \mathbf{G}_{E_i} \widetilde{\mathbf{P}}_{E_i} \mathbf{G}_{E_i}^H \right)^{-1}, \quad \forall k, \\ \widetilde{\mathbf{H}} &= \mathbf{H} - \lambda \mathbf{I}_{N_B}, \quad \mathbf{H} = \sum_{k=1}^K \mu_k \varepsilon_k \mathbf{H}_{E_k}^H \mathbf{H}_{E_k} + \beta \mathbf{h}_{I_R} \mathbf{h}_{I_R}^H, \\ \epsilon_S &= \lambda \tau_0 P_B + \beta \sigma_n^2 \tau_0 (1 - 2^{R_I/\tau_0}). \end{aligned} \quad (15)$$

Here,  $\{\lambda, \beta, \mu_k, \forall k\}$  are the non-negative lagrangian multipliers corresponding to constraints CR1, CR2 and CR3 in the problem (13), respectively. While  $\mathbf{Z}_0 \succeq \mathbf{0}$  and  $\mathbf{Z}_k \succeq \mathbf{0}, \forall k$  are the lagrangian multipliers corresponding to  $\widetilde{\mathbf{W}}_B \succeq \mathbf{0}$  and  $\widetilde{\mathbf{P}}_{E_k} \succeq \mathbf{0}, \forall k$ , respectively.  $\mathbf{M}_{\mathcal{K} \setminus k}^{\frac{1}{2}}$  denotes the Hermitian square root of the positive definite matrix  $\mathbf{M}_{\mathcal{K} \setminus k}$ . Since the problem (13) is concave, its Karush-Kuhn-Tucker (KKT) conditions are necessary and sufficient for the optimal solution. Based on the KKT conditions and the definitions  $\widetilde{\mathbf{W}}_B = \tau_0 \mathbf{W}_B$  and  $\widetilde{\mathbf{P}}_{E_k} = (1-\tau_0) \mathbf{P}_{E_k}, \forall k \in \mathcal{K}$ , the optimal beamforming and lagrangian multipliers should follow the structure shown in the following theorem.

**Theorem 1.** For any given time splitting ratio  $\tau_0$ , the optimal lagrangian multipliers  $\lambda^*, \beta^*, \mu_k^*, \forall k$ , the optimal downlink beamforming  $\mathbf{W}_B^*$  and the optimal uplink beamforming  $\mathbf{P}_{E_k}^*, \forall k$  to the problem (13) are expressed as

$$(\mathbf{W}_B^*, \lambda^*) = \begin{cases} (P_B \mathbf{u}_H \mathbf{u}_H^H, \lambda_H^{\max}) & 0 \leq R_I < R_I^{up} \\ (\frac{P_B}{\|\mathbf{h}_{I_R}\|^2} \mathbf{h}_{I_R} \mathbf{h}_{I_R}^H, 0) & R_I = R_I^{up} \end{cases}, \quad (16a)$$

$$\mathbf{P}_{E_k}^* = \mathbf{V}_{\mathcal{M}_{\mathcal{K} \setminus k}}^* \Lambda_{P_{E_k}} \mathbf{V}_{\mathcal{M}_{\mathcal{K} \setminus k}}^{*H}, \quad (16b)$$

$$\Lambda_{P_{E_k}} = \text{diag}[\Lambda_{P_{E_k},1}, \dots, \Lambda_{P_{E_k},N_U}] \quad (16c)$$

$$\Lambda_{P_{E_k},i} = \left[ \frac{1}{\ln 2 \mu_k^*} - \frac{\sigma_n^2}{\Lambda_{\mathcal{M}_{\mathcal{K} \setminus k},i}^2} \right]^+, \quad \forall i, \forall k, \quad (16d)$$

$$\mu_k^* = \frac{N_U (1-\tau_0)}{\ln 2 \left( \tau_0 \varepsilon_k \text{tr}(\mathbf{H}_{E_k} \mathbf{W}_B^* \mathbf{H}_{E_k}^H) + \sum_{i=1}^{N_U} \frac{(1-\tau_0) \sigma_n^2}{\Lambda_{\mathcal{M}_{\mathcal{K} \setminus k},i}^2} \right)}, \quad (16e)$$

$$\beta^* = \begin{cases} 0 & 0 \leq R_I \leq R_I^{mi} \\ \arg \{f_R(\mathbf{W}_B^*) = R_I\} & R_I^{mi} < R_I < R_I^{up} \\ +\infty & R_I = R_I^{up} \end{cases}, \quad (16f)$$

where  $\lambda_H^{\max}$  and  $\mathbf{u}_H$  are the maximum eigenvalue and the corresponding dominated eigenvector of  $\mathbf{H}^* = \sum_{k=1}^K \mu_k^* \varepsilon_k \mathbf{H}_{E_k}^H \mathbf{H}_{E_k} + \beta^* \mathbf{h}_{I_R} \mathbf{h}_{I_R}^H$ , respectively,  $\mathbf{V}_{\mathcal{M}_{\mathcal{K} \setminus k}}^*$  is defined as the  $N_U$ -dimensional right singular matrix of  $\mathbf{M}_{\mathcal{K} \setminus k}^{\frac{1}{2}} \mathbf{G}_{E_k}$  based on the singular value decomposition (SVD)  $\mathbf{M}_{\mathcal{K} \setminus k}^{\frac{1}{2}} \mathbf{G}_{E_k} = \mathbf{U}_{\mathcal{M}_{\mathcal{K} \setminus k}}^* \Lambda_{\mathcal{M}_{\mathcal{K} \setminus k}}^* \mathbf{V}_{\mathcal{M}_{\mathcal{K} \setminus k}}^{*H}, \forall k$ , and the diagonal matrix  $\Lambda_{\mathcal{M}_{\mathcal{K} \setminus k}}^* = \text{diag}[\Lambda_{\mathcal{M}_{\mathcal{K} \setminus k},1}^*, \dots, \Lambda_{\mathcal{M}_{\mathcal{K} \setminus k},N_U}^*]$  consists of  $N_U$  singular values

of  $M_{\mathcal{K} \setminus k}^{\star \frac{1}{2}} \mathbf{G}_{E_k}$ . In addition,  $f_R(\mathbf{W}_B^*)$  denotes the achievable downlink rate function as  $f_R(\mathbf{W}_B^*) = \tau_0 \log(1 + \sigma_n^{-2} \mathbf{h}_{I_R}^H \mathbf{W}_B^* \mathbf{h}_{I_R})$ .

*Proof.* Please see Appendix B.  $\square$

Theorem 1 provides the semi-closed-form optimal solutions for the problem (13). By iteratively solving from the lagrangian multipliers as well as the downlink and uplink beamforming based on (16a)-(16f), the optimal solution can be obtained. The convergence of the iterative calculation and the global optimality of the obtained solution are also guaranteed since the problem (13) is jointly concave. Moreover, from Theorem 1, we have the following insightful observations.

1) The optimal downlink beamforming  $\mathbf{W}_B^*$  is a rank-1 matrix, whose eigenspace is uniquely determined by the dominant eigenvector in the joint eigenspace spanned by  $K$  ERs' downlink channels  $\mathbf{H}_{E_k}, \forall k \in \mathcal{K}$  and the IR's downlink channel  $\mathbf{h}_{I_R}$ . Since SWIPT is conducted in the downlink, the downlink beamforming should provide a good balance between energy transfer and information transmission. Whether the optimal downlink beamforming aligns toward the space of the ERs' channels for energy transfer or that of the IR's channel for information transmission is controlled by the lagrangian multipliers  $\{\mu_k^*, \forall k \in \mathcal{K}, \beta^*\}$  and depends on the downlink rate constraint. Specifically, when the downlink rate constraint is not high, i.e.,  $0 \leq R_I \leq R_I^{mi}$ ,  $\beta^* = 0$  holds and the optimal downlink beamforming is fully aligned with the eigenspace of the ERs' channels. In other words, the optimal downlink beamforming is designed only aiming at energy transfer while ignoring the need of information transmission since the required information transmission can be automatically satisfied.

However, when the downlink rate constraint is high, i.e.,  $R_I^{mi} < R_I < R_I^{up}$ , we have  $\beta^* = \arg \{f_R(\mathbf{W}_B^*) = R_I\}$ , the need for information transmission cannot be ignored and the optimal downlink beamforming shifts from the space of the ERs' channels toward that of the IR's channel. When the downlink rate constraint is as high as the maximum rate  $R_I = R_I^{up}$ ,  $\beta^* = +\infty$  and the downlink beamforming should be fully aligned with the IR's channel to meet the strict information transmission requirement. To some extent, the optimal lagrangian multiplier  $\beta^*$  therefore can be regarded as an indicator of the relativity between the downlink beamforming and the IR's downlink channel. High  $\beta^*$  means high relativity between the optimal downlink beamforming and the IR's downlink channel.

2) It is seen from (16b)~(16e) that the optimal uplink beamforming  $\mathbf{P}_{E_k}^*$  depends on the downlink beamforming  $\mathbf{W}_B^*$  through the lagrangian multiplier  $\mu_k^*$ . This is due to the fact that the uplink transmission energy in each ER is constrained by its energy harvested in the downlink, i.e., the constraint CR3. Moreover, the optimal uplink beamforming  $\mathbf{P}_{E_k}^*$  for the  $k$ th ER  $E_k$  is related to other ERs' uplink beamforming, i.e.,  $\{\mathbf{P}_{E_i}^*, \forall i \neq k\}$ , through the matrix  $\mathbf{M}_{\mathcal{K} \setminus k}^*$ . To solve for the coupled uplink beamforming  $\{\mathbf{P}_{E_k}^*, \forall k\}$  in (16b), the iterative water-filling procedure [27] can be applied. With the concavity of the problem (13), the iterative water-filling procedure is guaranteed to converge to the globally

optimal  $\{\mathbf{P}_{E_k}^*, \forall k\}$ . Interested readers can refer to [27] for the detailed iterative process.

3) When  $R_I^{mi} < R_I < R_I^{up}$ , the optimal lagrangian multiplier  $\beta^*$  is determined by the nonlinear function  $f_R(\mathbf{W}_B^*)$ . After analysis, we find the function  $f_R(\mathbf{W}_B)$  has the monotonically increasing property as follows.

**Lemma 2.** *Given the downlink beamforming structure  $\mathbf{W}_B = P_B \mathbf{u}_H \mathbf{u}_H^H$  in (16a), the function  $f_R(\mathbf{W}_B)$  is monotonically increasing w.r.t.  $\beta \in (0, +\infty)$  and converges to  $R_I^{up}$  when  $\beta \rightarrow +\infty$ .*

*Proof.* Please see Appendix C.  $\square$

Based on Lemma 2, the optimal  $\beta^*$  satisfying  $f_R(\mathbf{W}_B^*) = R_I$  can be uniquely determined by the bisection search. Now with the semi-closed-form optimal solution in Theorem 1 for the problem (13), our remaining task is to find the optimal time splitting ratio  $\tau_0$  to achieve the maximum uplink sum rate. Mathematically, it is to solve the problem  $\tau_0^* = \arg \max_{0 \leq \tau_0 \leq 1} f_S(\tau_0)$ . Since the objective function  $f_S(\tau_0)$  is concave w.r.t.  $\tau_0$ , the Golden section search can be utilized to find the globally optimal  $\tau_0$  [29].

## B. TDMA-enabled uplink sum rate maximization

Due to the involvement of additional uplink time allocation vector, the TDMA-enabled uplink sum rate maximization in (12) is more challenging than the problem (11). As far as we know, the joint design of beamforming and time allocation vector for TDMA-enabled WPSNs is rarely discussed in the literature. Here we will follow a similar approach as that for SDMA-enabled WPSNs to solve this challenging problem. To be specific, by fixing the time splitting ratio  $\tau_0$ , the problem (12) can be rewritten as

$$\begin{aligned} f_T(\tau_0) = & \max_{\substack{\tau_{up}, \tilde{\mathbf{W}}_B \succeq \mathbf{0}, \\ \tilde{\mathbf{P}}_{E_k} \succeq \mathbf{0}, \forall k}} \sum_{k=1}^K \tau_{E_k} \log \det(\mathbf{I}_{N_B} + \frac{\sigma_n^{-2}}{\tau_{E_k}} \mathbf{G}_{E_k} \tilde{\mathbf{P}}_{E_k} \mathbf{G}_{E_k}^H) \\ & + \tau_{I_R} \log \det(\mathbf{I}_{N_B} + \sigma_n^{-2} P_I \mathbf{g}_{I_R} \mathbf{g}_{I_R}^H) \\ \text{s.t. } & \widetilde{\text{CR1}}, \widetilde{\text{CR2}}, \widetilde{\text{CR3}}, \text{CR5}. \end{aligned} \quad (17)$$

where  $\tau_{up} = [\tau_{E_1}, \dots, \tau_{E_K}, \tau_{I_R}]$  denotes the uplink time allocation. Clearly, the problem (17) is jointly concave w.r.t.  $\{\tau_{up}, \tilde{\mathbf{W}}_B, \tilde{\mathbf{P}}_{E_k}, \forall k\}$ , and the corresponding Lagrangian function is expressed as

$$\begin{aligned} L_T(\mathcal{A}_T) = & \sum_{k=1}^K \tau_{E_k} (\log \det(\mathbf{I}_{N_B} + \frac{\sigma_n^{-2}}{\tau_{E_k}} \mathbf{G}_{E_k} \tilde{\mathbf{P}}_{E_k} \mathbf{G}_{E_k}^H) - \gamma) \\ & + \text{tr} \left( (\tilde{\mathbf{H}} + \mathbf{Z}_0) \tilde{\mathbf{W}}_B \right) - \sum_{k=1}^K \text{tr}((\mu_k \mathbf{I}_{N_U} - \mathbf{Z}_k) \tilde{\mathbf{P}}_{E_k}) \\ & + \tau_{I_R} (C_R - \gamma) + \epsilon_T. \end{aligned} \quad (18)$$

where  $\mathcal{A}_T = \{\tau_{up}, \tilde{\mathbf{W}}_B, \tilde{\mathbf{P}}_{E_k}, \lambda, \beta, \gamma, \mathbf{Z}_0, \mathbf{Z}_k, \mu_k, \forall k\}$ ,  $C_R = \log \det(\mathbf{I}_{N_B} + \sigma_n^{-2} P_I \mathbf{g}_{I_R} \mathbf{g}_{I_R}^H)$  is a constant denoting the spectral efficiency of the IR's uplink channel, and  $\epsilon_T = \epsilon_S - \gamma(\tau_0 - 1)$ . Here,  $\{\lambda, \beta, \mu_k, \forall k, \gamma\}$  denote the non-negative lagrangian multipliers corresponding to the constraints CR1, CR2, CR3 and CR5 in the problem (17), respectively.  $\mathbf{Z}_0 \succeq \mathbf{0}$  and  $\mathbf{Z}_k \succeq$

$\mathbf{0}, \forall k$  are still the lagrangian multipliers corresponding to  $\bar{\mathbf{W}}_B \succeq \mathbf{0}$  and  $\bar{\mathbf{P}}_{E_k} \succeq \mathbf{0}, \forall k$ , respectively. With the concavity of the problem (17) and based on its KKT conditions, the optimal structures for the variables  $\{\tau_{up}, \mathbf{W}_B, \mathbf{P}_{E_k}, \lambda, \beta, \gamma, \mu_k, \forall k\}$  can be derived in the following theorem.

**Theorem 2.** For any given time splitting ratio  $\tau_0$ , the optimal  $\{\mathbf{W}_B^*, \lambda^*, \beta^*\}$  to the problem (17) are identical to that in Theorem 1, while the optimal  $\tau_{up}^*$  and  $\mathbf{P}_{E_k}^*, \forall k$  to the problem (17) as well as the optimal lagrangian multipliers  $\mu_k^*, \forall k, \gamma^*$ , are given by

$$\mathbf{P}_{E_k}^* = \mathbf{V}_{G_{E_k}} \mathbf{\Lambda}_{P_{E_k}} \mathbf{V}_{G_{E_k}}^H / \tau_{E_k}^*, \quad (19a)$$

$$\mathbf{\Lambda}_{P_{E_k}} = \text{diag}[\Lambda_{P_{E_k},1}, \dots, \Lambda_{P_{E_k},N_U}] \quad (19b)$$

$$\Lambda_{P_{E_k},i} = \left[ \frac{\tau_{E_k}^*}{\ln 2 \mu_k^*} - \frac{\sigma_n^2 \tau_{E_k}^*}{\Lambda_{G_{E_k},i}^2} \right]^+, \quad i = 1, \dots, N_U \quad (19c)$$

$$\mu_k^* = \frac{N_U \tau_{E_k}^*}{\ln 2 \left( \tau_0 \varepsilon_k \text{tr}(\mathbf{H}_{E_k} \mathbf{W}_B^* \mathbf{H}_{E_k}^H) + \sum_{i=1}^{N_U} \frac{\sigma_n^2 \tau_{E_k}^*}{\Lambda_{G_{E_k},i}^2} \right)}, \quad \forall k, \quad (19d)$$

$$\tau_{up}^* = \begin{cases} \arg \left\{ \begin{aligned} & \left\{ \begin{aligned} & g_T(\tau_{E_k}) = \gamma^* \\ & \sum_{k=1}^K (\tau_{E_k})^+ = 1 - \tau_0 \\ & \tau_{IR} = 0 \end{aligned} \right\} \\ & [(\tau_{E_k})^+, \forall k, 0] \end{aligned} \right\} & \gamma^* > C_R \\ \arg \left\{ \begin{aligned} & \left\{ \begin{aligned} & g_T(\tau_{E_k}) = C_R \\ & \sum_{k=1}^K (\tau_{E_k})^+ + \tau_{IR} = 1 - \tau_0 \\ & \tau_{IR} > 0 \end{aligned} \right\} \\ & [(\tau_{E_k})^+, \forall k, \tau_{IR}] \end{aligned} \right\} & \gamma^* = C_R \end{cases} \quad (19e)$$

where  $\mathbf{V}_{G_{E_k}} \in \mathbb{C}^{N_U \times N_U}, \forall k$  is the right singular matrix of  $\mathbf{G}_{E_k}$  by performing the SVD  $\mathbf{G}_{E_k} = \mathbf{U}_{G_{E_k}} \mathbf{\Lambda}_{G_{E_k}} \mathbf{V}_{G_{E_k}}^H$ , the diagonal matrix  $\mathbf{\Lambda}_{G_{E_k}} = \text{diag}[\Lambda_{G_{E_k},1}, \dots, \Lambda_{G_{E_k},N_U}]$  consists of  $N_U$  singular values of  $\mathbf{G}_{E_k}, \forall k$ , and the function  $g_T(\tau_{E_k}) = \sum_{i=1}^{N_U} \left( \log \left( 1 + \frac{\sigma_n^{-2} \Lambda_{G_{E_k},i}}{\tau_{E_k}} \right) - \frac{\sigma_n^{-2} \Lambda_{G_{E_k},i}}{\ln 2 (\tau_{E_k} + \sigma_n^{-2} \Lambda_{G_{E_k},i})} \right)$  is defined with  $\Lambda_{G_{E_k},i} = \Lambda_{G_{E_k},i}^2 \Lambda_{P_{E_k},i}, \forall i = 1, \dots, N_U$ .

*Proof.* Please see Appendix D.  $\square$

From Theorem 2, we also have the following insightful observations.

1) Since both SDMA-enabled WPSNs and TDMA-enabled WPSNs have the same downlink transmission stage, the optimal downlink beamforming  $\mathbf{W}_B^*$  for TDMA-enabled uplink sum rate maximization has the same form as that for SDMA-enabled uplink sum rate maximization. Thus the insightful results on  $\{\mathbf{W}_B^*, \beta^*\}$  for SDMA-enabled WPSNs is also applicable for TDMA-enabled WPSNs.

2) From (19a)~(19d), we can see that the optimal uplink beamforming  $\mathbf{P}_{E_k}^*$  at the  $k$ th ER depends on the downlink beamforming  $\mathbf{W}_B^*$ , but is independent to the uplink beamforming of other ERs, i.e.,  $\{\mathbf{P}_{E_i}^*, \forall i \neq k\}$ . This is due to the fact that dedicated time slot is allocated to each ER for uplink transmission in TDMA-enabled WPSNs and thus the uplink beamforming design for each ER can be decoupled.

3) Additional uplink time allocation is required in TDMA-enabled WPSNs. As shown in (19e), to maximize the uplink sum rate, there are two possible uplink time allocations

depending on the channel conditions of all sensor nodes. Particularly, the function  $g_T(\tau_{E_k})$  can also be roughly regarded as the uplink spectral efficiency of the  $k$ th ER. Since the uplink spectral efficiency of IR is a constant as  $C_R = \log \det(\mathbf{I}_{N_B} + \sigma_n^{-2} P_{IR} \mathbf{g}_{IR} \mathbf{g}_{IR}^H)$ , the optimization of the uplink time slot  $\tau_{IR}$  for IR is actually a linearly constrained linear programming problem. Specifically, when the spectral efficiencies of all ERs  $g_T(\tau_{E_k}^*)$  are higher than that of the IR  $C_R$ , it is naturally to allocate the total uplink time resource (i.e.,  $1 - \tau_0$ ) only to the ERs, which are presented in the case of  $\gamma^* > C_R$  in (19e), while no time slot is allocated to the IR, namely  $\tau_{IR}^* = 0$ . Otherwise, in order to guarantee the nonzero uplink time allocation  $\tau_{IR}^*$  for the IR, there is at least a ER achieving the same spectral efficiency as that of the IR, namely,  $g_T(\tau_{E_k}^*) = C_R$ . Thus the total uplink time resource (i.e.,  $1 - \tau_0$ ) is optimally allocated as that in the case of  $\gamma^* = C_R$  of (19e). Overall, for both two cases, the uplink time allocation is somehow similar to the water-filling procedure and the spectral efficiency can be regarded as water level to be optimized higher than or equal to  $C_R$ . To find the optimal uplink time allocation, the nonlinear equation  $g_T(\tau_{E_k}) = \gamma^*$  needs to be solved. Fortunately, the function  $g_T(\tau_{E_k})$  has the following property which can facilitate the derivation of the optimal time slot  $\tau_{E_k}$ .

**Lemma 3.** The function  $g_T(\tau_{E_k})$  is monotonically decreasing w.r.t.  $\tau_{E_k} > 0, \forall k$ .

*Proof.* Taking the first order derivation of  $g_T(\tau_{E_k})$  on  $\tau_{E_k}$ , we have  $\nabla_{\tau_{E_k}} g_T(\tau_{E_k}) = \sum_{i=1}^{N_U} \frac{-(\sigma_n^{-2} \Lambda_{G_{E_k},i})^2}{\ln 2 (\tau_{E_k} + \sigma_n^{-2} \Lambda_{G_{E_k},i})^2 \tau_{E_k}}$ . It is readily observed that for  $\tau_{E_k} > 0$ , we have  $\nabla_{\tau_{E_k}} g_T(\tau_{E_k}) < 0, \forall k$ . Therefore, the function  $g_T(\tau_{E_k}), \forall k$  is monotonically decreasing w.r.t.  $\tau_{E_k} > 0$ .  $\square$

With the monotonicity of  $g_T(\tau_{E_k})$ , the solution of  $g_T(\tau_{E_k}) = \gamma^*$  can be uniquely determined. Moreover, since  $l_T(\tau_{E_k}, \forall k) = \sum_{k=1}^K \tau_{E_k}$  is also monotonically increasing w.r.t.  $\tau_{E_k}, \forall k$ , the optimal solution  $\tau_{up}^*$  and the optimal  $\gamma^*$  in (19e) can be efficiently obtained by the iterative bisection search (IBS) [28].

Similarly to the problem (13), Theorem 2 also provides a semi-closed-form optimal solution for the problem (17) with a given  $\tau_0$ . Since the objective function  $f_T(\tau_0)$  is also concave w.r.t.  $\tau_0$ , the Golden section search can still be applied to find the optimal time splitting ratio  $\tau_0^*$  satisfying  $\tau_0^* = \arg \max_{0 \leq \tau_0 \leq 1} f_T(\tau_0)$ .

### C. Summary and discussion

For clarification, the implementation of the proposed semi-closed-form optimal solutions for both SDMA-enabled and TDMA-enabled uplink sum rate maximization is summarized as Algorithm 1 & 2. Specifically, the Golden section search for the optimal time splitting ratio  $\tau_0^*$  is shown in Algorithm 1, while the semi-closed-form solutions for the SDMA-enabled problem (13) and the TDMA-enabled problem (17) are illustrated in Algorithm 2.



**Algorithm 1** Optimization of the time splitting ratio  $\tau_0$ 

- 
- 1: Initialize:  $\tau_{min} = 0$ ,  $\tau_{max} = 1$  and step  $\phi = (\sqrt{5} - 1)/2$
  - 2: **repeat**
  - 3:   Calculate  $\tau_1 = \tau_{max} - (\tau_{max} - \tau_{min})\phi$  and  $\tau_2 = \tau_{min} + (\tau_{max} - \tau_{min})\phi$ .
  - 4:   Obtain  $f_{S/T}(\tau_1)$  and  $f_{S/T}(\tau_2)$  from Algorithm 2.
  - 5:   **if**  $f_{S/T}(\tau_1) > f_{S/T}(\tau_2)$ , set  $\tau_{max} = \tau_2$ .
  - 6:   **else** set  $\tau_{min} = \tau_1$ .
  - 7: **until**  $|\tau_{max} - \tau_{min}| \leq \kappa$ , where  $\kappa > 0$  is sufficiently small.
  - 8: **return** the optimal  $\tau_0^* = (\tau_{max} + \tau_{min})/2$
- 

**Algorithm 2** Semi-closed-form solutions in Theorem 1 and Theorem 2

- 
- 1: Input:  $\tau_0 = \tau_1/\tau_2$ ; initial  $\mu_k^{(0)}$ ,  $\mathbf{P}_{E_k}^{(0)} = \mathbf{0}, \forall k$  and  $\tau_{up}^{(0)}$ ; iteration index  $i=0$ .
  - 2: **repeat**
  - 3:   Given  $\mu_k^{(i)}, \forall k$ , apply the bisection search to (16f) to find  $\beta^{(i)}$ , then  $\mathbf{W}_B^{(i)}$  is obtained from (16a).
  - 4:   **if** (SDMA-enabled WPSN is considered)
  - 5:    Given  $\mathbf{W}_B^{(i)}$ , apply the iterative water-filling procedure to obtain  $\mathbf{P}_{E_k}^{(i)}$  and  $\mu_k^{(i+1)}, \forall k$  from (16b)~(16e).
  - 6:    **elseif** (TDMA-enabled WPSN is considered)
  - 7:    Given  $\mathbf{W}_B^{(i)}, \tau_{up}^{(i)}$ , obtain  $\mathbf{P}_{E_k}^{(i)}$  and  $\mu_k^{(i+1)}, \forall k$  from (19b)~(19d).
  - 8:    Given  $\mathbf{P}_{E_k}^{(i)}, \forall k$ , obtain  $\tau_{up}^{(i)}$  from (19e).
  - 9:   **end**
  - 10:   Calculate  $f_{S/T}^{(i)}(\tau_0)$  and update  $i=i+1$ ;
  - 11: **until**  $f_{S/T}^{(i)}(\tau_0)$  converges.
  - 12: **return** Optimal  $\mathbf{W}_B^{(i)}, \tau_{up}^{(i)}, \mathbf{P}_{E_k}^{(i)}, \forall k, f_{S/T}^{(i)}(\tau_0)$ .
- 

Since the problems (7) and (9) are jointly concave on  $\{\tau_0, \mathbf{W}_B, \mathbf{P}_{E_k}, \forall k\}$  and  $\{\tau, \mathbf{W}_B, \mathbf{P}_{E_k}, \forall k\}$ , respectively, their KKT conditions are sufficient and necessary for the globally optimal solutions no matter whether  $\tau_0$  is given. Therefore the semi-closed-form solutions derived based on KKT conditions in Theorem 1 and 2 are globally optimal. In other words, Algorithm 2 is guaranteed to converge to the global optimal solutions for both SDMA-enabled problem (13) and the TDMA-enabled problem (17). Meanwhile, with the concavity of the objective functions  $f_{S/T}(\tau_0)$  w.r.t.  $\tau_0$ , the global optimality of the obtained  $\tau_0^*$  from Algorithm 1 is also assured. As a result, our proposed algorithm is guaranteed to converge to the globally optimal solutions for both SDMA-enabled and TDMA-enabled uplink sum rate maximizations.

Although iterative calculations are required in our proposed algorithm, the complexity of our proposed algorithm with semi-closed-form solutions is still lower than that of the traditional numerical algorithms for standard convex problems, such as, the interior point method. Here, we take the SDMA-enabled WPSN as an example for complexity analysis. As shown in Algorithm 1&2, Golden section search, bisection search, iterative water-filling procedure and SVD/EVD operations are clearly involved. By denoting the converged numbers of iterations for the first three processes as  $I_G$ ,  $I_B$  and  $I_W$ , respectively, the complexity of our proposed algorithm can be

expressed as  $I_G I_{semi} (I_W \mathcal{O}(KN_U^3) + I_B + \mathcal{O}(N_B^3))$ , where  $I_{semi}$  denotes the number of iterations in Algorithm 2 and  $\mathcal{O}(n^3)$  denotes the complexity of SVD/EVD operations. It is well-known that Golden section search and the bisection search are efficient with small numbers of iterations. Mathematically, we have  $I_G = \log_2(\frac{1}{\epsilon})$  and  $I_B = \log_2(\frac{\beta_{max}}{\epsilon})$ , where  $\epsilon$  denotes the search accuracy [29]. In addition, the iterative water-filling procedure usually converges fast with small  $I_W$  [27] and the number of iterations  $I_{semi}$  of Algorithm 2 is also small as shown in the simulations. Nevertheless, by referring to [30] and recalling the original jointly concave problem (11), which is like a SDP problem due to the positive semidefinite optimization variables, the corresponding complexity of the numerical interior point method is  $\mathcal{O}(K(KN_U + N_B)^{3.5} + K^2(KN_U + N_B)^{2.5} + K^3(KN_U + N_B)^{0.5}) \log(1/\epsilon)$  [30]. Clearly, our proposed algorithm has much lower complexity than the numerical convex algorithm, not to mention the meaningful insights found from our semi-closed-form solutions.

Last but not least, due to the additional practical consideration of the downlink rate constraint in partially WPSNs, our joint downlink and uplink beamforming designs as well as time splitting are remarkably different from that in most of the existing works. Particularly, our SDMA-enabled design in fact reduces to that in [17] when the downlink rate constraint is not tight. While for the TDMA-enabled WPSNs, due to another additional involvement of uplink time allocation, the joint beamforming design and time splitting is more challenging and rarely discussed in the literature. However, our proposed semi-closed-form design provides the optimal solutions with low complexity for this challenging problem.

## V. SIMULATION RESULTS AND DISCUSSIONS

In this section, simulation results are provided to demonstrate the effectiveness of the proposed uplink sum rate maximizations for the SDMA-enabled and TDMA-enabled MIMO WPSNs, respectively. Unless otherwise stated, we consider one H-AP with  $N_B = 6$  antennas,  $K = 3$  ERs each with  $N_U = 3$  antennas and one IR with single antenna. Besides, the H-AP is assumed to locate at the origin (0,0)m, while the three ERs and one IR are randomly located within a circle with radius 10m. All wireless channels are generated according to Rayleigh distribution  $\mathcal{CN}(\mathbf{0}, 10^{-3}d^{-\alpha}\mathbf{I})$ , where  $d$  denotes the actual distance between the H-AP and ERs/IR, and  $\alpha = 3$  is the pathloss exponent. In addition, the received Gaussian noise variance is set to be  $\sigma_n^2 = -100$ dBm. The maximum downlink and uplink transmit powers of H-AP and IR are defined as  $P_B = 20$ dBm and  $P_I = 5$ dBm, respectively. Here we adopt two benchmark designs for comparisons. One is the maximum downlink rate (MDR) based beamforming scheme where the downlink beamforming is fixed as  $\mathbf{W}_B^{up} = \frac{P_B}{\|\mathbf{h}_{IR}\|^2} \mathbf{h}_{IR} \mathbf{h}_{IR}^H$ , while the other is the proposed uplink sum rate optimization with fixed time allocation  $\tau_0 = 0.5$ , which indicates equal time splitting for downlink and uplink transmissions.

The optimal time splitting  $\tau_0$  and the optimal downlink and uplink beamformings are obtained through Golden section search and iterative optimization procedure, respectively, as shown in Algorithms 1 & 2. We first investigate the convergence of the proposed iterative optimization procedure in



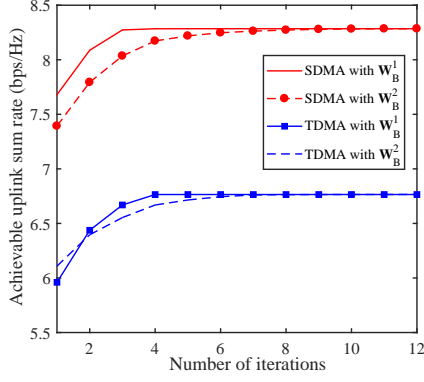


Fig. 2. Convergence of Algorithm 2 for both WPSNs, where  $R_I = R_I^0$  and  $\tau_0 = 0.5$ .

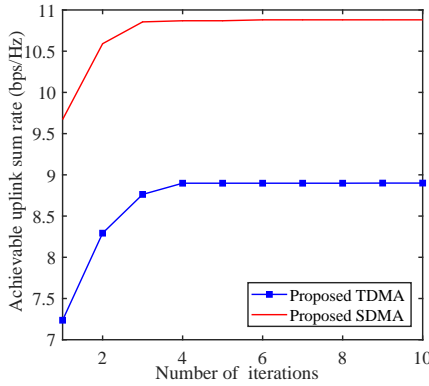


Fig. 3. Convergence of Algorithm 1 for both WPSNs, where  $R_I = R_I^0$ .

Algorithm 2, where  $\tau_0 = 0.5$  and  $R_I = R_I^0$  satisfying  $R^{mi} < R_I^0 \leq R^{up}$  are defined. In particular, two initial values of  $\mathbf{W}_B$  are adopted as follows:

$$\begin{aligned} \mathbf{W}_B^1 &= \frac{P_B}{N_B} \mathbf{I}_{N_B}; \quad \mathbf{W}_B^2 = \mathbf{a}\mathbf{a}^H, \\ |\mathbf{h}_{IR}^H \mathbf{a}|^2 &= \sigma_n^2 (2^{\frac{R_I^0}{\tau_0}} - 1), \quad \|\mathbf{a}\|^2 = P_B. \end{aligned} \quad (20)$$

The results are shown in Fig. 2. It is clear that using both initial  $\mathbf{W}_B$  in (20), the proposed iterative optimization procedure converges to the maximum uplink sum rate within 8 iterations for both SDMA-enabled and TDMA-enabled WPSNs with fixed time splitting  $\tau_0 = 0.5$ . Then Fig. 3 shows the convergence of Golden section search in Algorithm 1 for finding the optimal  $\tau_0$ . It is also clearly seen that for both WPSNs, the achievable maximum uplink sum rate converges within 5 iterations.

In Fig. 4, the achievable uplink sum rate versus the H-AP transmit power  $P_B$  is studied for all three considered schemes in both SDMA-enabled and TDMA-enabled WPSNs. Here,  $R_I = \frac{R^{mi}}{2}$  is assumed, which means that the downlink rate constraint is inactive for both SDMA-enabled and TDMA-enabled uplink sum rate maximization. Under this setting, the proposed SDMA-enabled uplink sum rate maximization is actually reduced to the sum throughput maximization for fully WPSNs in [17]. It is observed from Fig. 4 that the

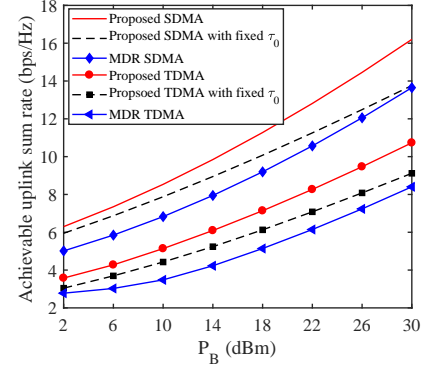


Fig. 4. Achievable uplink sum rate versus H-AP transmit power  $P_B$  for both WPSNs, where  $R_I = \frac{R^{mi}}{2}$ .

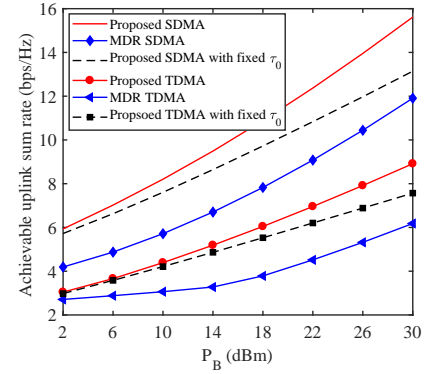


Fig. 5. Achievable uplink sum rate versus H-AP transmit power  $P_B$  for both WPSNs, where  $R_I = R_I^1$  and  $R^{mi} < R_I^1 \leq 0.5 R^{up}$ .

achievable uplink sum rate increases with the H-AP transmit power  $P_B$  for all considered schemes. Besides, it is clear that the SDMA based scheme generally achieves higher uplink sum rate than the corresponding TDMA based scheme due to the simultaneous uplink transmission from all the ERs and IR. By comparing the proposed SDMA/TDMA scheme with the corresponding counterpart with fixed  $\tau_0 = 0.5$ , we also find that the time splitting optimization plays an important role in improving uplink sum rate for both SDMA-enabled and TDMA-enabled WPSNs. Additionally, the MDR SDMA/TDMA scheme performs worst among three SDMA/TDMA schemes due to the fact that most H-AP transmit power is utilized for downlink information transmission, which thus results in limited harvested energy at ERs for uplink transmission.

We then extend this simulation to the case with the downlink threshold  $R_I = R_I^1$  where  $R^{mi} < R_I^1 \leq 0.5 R^{up}$  is defined to guarantee the feasibility of the proposed SDMA/TDMA scheme with fixed  $\tau_0 = 0.5$  and the results are shown in Fig. 5. Notice that under  $R^{mi} < R_I^1 \leq 0.5 R^{up}$ , the downlink rate constraint is tight and will affect the achievable sum rate and the optimal solutions. Similar results to that in Fig. 4 can also be observed from Fig. 5. Moreover, we also find that for all considered schemes, the achievable uplink sum rate in Fig. 5 is naturally lower than that in Fig. 4 under a given  $P_B$ , since the

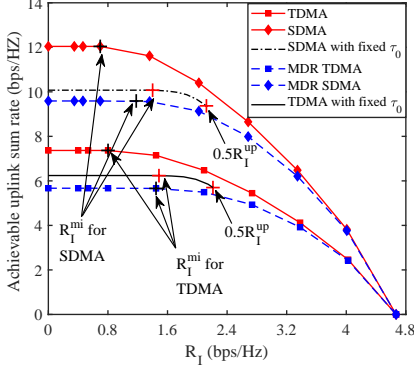


Fig. 6. Achievable uplink sum rate versus downlink rate threshold  $R_I$  for both WPSNs.

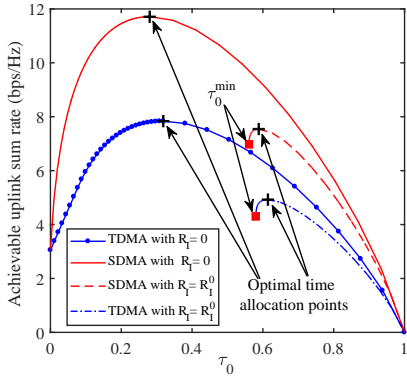


Fig. 7. Achievable uplink sum rate versus downlink time duration  $\tau_0$  for both WPSNs, where both  $R_I = 0$  and  $R_I = R_I^0$  are considered.

uplink sum rate maximization for both WPSNs is constrained by a higher downlink rate threshold  $R_I = R_I^1$  in Fig. 5.

In Fig. 6, we illustrate the achievable uplink sum rate as a function of the downlink rate threshold  $R_I$  for both SDMA-enabled and TDMA-enabled WPSNs. It is firstly seen that when  $0 \leq R_I \leq R_I^{mi}$ , the achievable uplink sum rate is flat, which indicates that the downlink rate constraint actually has no influence on the achievable uplink sum rate. Then when  $R_I^{mi} < R_I \leq R_I^{up}$ , the achievable uplink sum rate decreases with the increase of  $R_I$  implying the downlink rate constraint becomes tight. Moreover, we also find that for all three considered schemes, the SDMA-enabled WPSN has a larger uplink-downlink rate region compared to the TDMA-enabled WPSN. Taking the SDMA-enabled WPSN as an example, it is readily found that the proposed SDMA scheme with the optimized  $\tau_0$  still performs best, whereas the MDR SDMA scheme firstly realizes the lowest uplink sum rate and then approaches to the proposed SDMA scheme with the rise of  $R_I$ , since when  $R_I \rightarrow R_I^{up}$ , the optimal downlink beamforming  $\mathbf{W}_B^*$  of the proposed SDMA scheme also tends to be  $\mathbf{W}_B^{up} = \frac{\mathbf{P}_B}{\|\mathbf{h}_{IR}\|^2} \mathbf{h}_{IR} \mathbf{h}_{IR}^H$ . As for the proposed SDMA scheme with fixed  $\tau_0 = 0.5$ , the achievable maximum downlink rate is easily found to be  $0.5R_I^{up}$ . The above results also hold for the TDMA-enabled WPSN.

Fig. 7 finally depicts the achievable uplink sum rate as a

function of the downlink time duration  $\tau_0$  for both SDMA-enabled and TDMA-enabled WPSNs. Two downlink rate thresholds  $R_I = 0$  and  $R_I = R_I^0$  satisfying  $R_I^{mi} < R_I^0 \leq R_I^{up}$  are considered, respectively. It is clear from Fig. 7 that for both WPSNs, the achievable uplink sum rate  $f_S(\tau_0)/f_T(\tau_0)$  is indeed concave w.r.t.  $\tau_0$  under both thresholds  $R_I$ . Particularly, when  $R_I = 0$ , both WPSNs achieve the same uplink sum rate at the point  $\tau_0 = 0$  since only transmission from the energy-stable IR happens in the uplink. However, in the case of  $R_I = R_I^0$ , the minimum downlink time duration  $\tau_0^{min}$  is required to satisfy the downlink rate constraints of both WPSNs.

## VI. CONCLUSION

In this paper, we investigated the uplink sum rate maximization for both SDMA-enabled and TDMA-enabled partially WPSNs. Different from most existing WPSNs related works, the downlink simultaneous wireless information and power transfer was considered and downlink rate constraint was taken into account in our optimal design. After analyzing the downlink rate constraint and converting the original non-convex uplink sum rate maximization problems into concave ones, semi-closed-form optimal solutions for downlink beamforming, uplink beamforming and time allocation were proposed. Global optimality was proved and low complexity of the proposed optimal solutions were justified. Moreover, from the analysis we found that downlink rate constraint played a significant role and required special care in the optimal design. Finally, numerical simulations verified the excellent performance of the proposed uplink sum rate optimization schemes for both WPSNs.

## APPENDIX A

We can prove Lemma 1 by contradiction as follows. Firstly, given a downlink rate threshold  $R_I^1$  satisfying  $R_I^{mi} < R_I^1 \leq R_I^{up}$ , we denote the corresponding maximum objective value of the problem (7) as  $f_{obj, R_I^1}^*(\tau_{0,1}^*, \mathbf{P}_{E_{k,1}}^*, \mathbf{W}_{B,1}^*, \forall k)$ , where  $\tau_{0,1}^*$ ,  $\mathbf{W}_{B,1}^*$  and  $\mathbf{P}_{E_{k,1}}^*, \forall k$  are the optimal solutions to the problem (7) with the downlink rate threshold  $R_I = R_I^1$ . Meanwhile, we assume  $\tau_0 \log(1 + \sigma_n^{-2} \mathbf{h}_{IR}^H \mathbf{W}_{B,1}^* \mathbf{h}_{IR}) > R_I^1$ . Based on this assumption, it is readily concluded that when another downlink threshold  $R_I^2$  satisfying  $R_I^2 = \tau_0 \log(1 + \sigma_n^{-2} \mathbf{h}_{IR}^H \mathbf{W}_{B,1}^* \mathbf{h}_{IR}) > R_I^1$  is applied to the problem (7), the previous obtained solution  $\mathbf{Q}_1 = \{\tau_{0,1}^*, \mathbf{W}_{B,1}^*, \mathbf{P}_{E_{k,1}}^*, \forall k\}$  actually becomes a feasible solution for the problem (7) with  $R_I = R_I^2$ , since all the constraints are satisfied. So we have

$$f_{obj, R_I^1}^*(\mathbf{Q}_1) \leq f_{obj, R_I^2}^*(\mathbf{Q}_2) \quad (21)$$

where  $\mathbf{Q}_2 = \{\tau_{0,2}^*, \mathbf{W}_{B,2}^*, \mathbf{P}_{E_{k,2}}^*, \forall k\}$  is the corresponding optimal solution to the problem (7) with  $R_I = R_I^2$ . On the other hand, since  $R_I^2 > R_I^1$ , the set of feasible solutions of the problem (7) with  $R_I = R_I^2$  becomes smaller than that with  $R_I = R_I^1$ , thus we have

$$f_{obj, R_I^1}^*(\mathbf{Q}_1) \geq f_{obj, R_I^2}^*(\mathbf{Q}_2). \quad (22)$$

By combining (21) and (22), it is readily concluded that

$$f_{obj, R_I^1}^*(\mathbf{Q}_1) = f_{obj, R_I^2}^*(\mathbf{Q}_2). \quad (23)$$

Similarly, for an arbitrary threshold  $R_I \in [R_I^1, R_I^2]$ , the same maximum objective value of the problem (7) can also be obtained, which implies that the downlink rate constraint actually does not affect the problem (7) and thus can be ignored. As discussed in Section III. B, this happens only when  $R_I^2 \leq R_I^{mi}$ , which contradicts with the original assumption of  $R_I^{mi} < R_I^1 < R_I^2 \leq R_I^{up}$ . Therefore, the initial assumption is invalid, we must have the optimal downlink beamforming located at the boundary, i.e.,  $\tau_0 \log(1 + \sigma_n^{-2} \mathbf{h}_{IR}^H \mathbf{W}_B^* \mathbf{h}_{IR}) = R_I$  for the problem (7) when  $R_I^{mi} < R_I \leq R_I^{up}$ . Secondly, since  $R_I^{mi}$  can be considered to be a critical point at which the downlink rate constraint becomes tight, we finally conclude that the downlink rate constraint is tight when  $R_I^{mi} \leq R_I \leq R_I^{up}$ . This completes the proof.

#### APPENDIX B

Firstly, we consider the special case of  $R_I = R_I^{up}$  for the problem (13), in which both the constraints  $\widetilde{\text{CR1}}$  and  $\widetilde{\text{CR2}}$  are not strictly feasible (must be tight) by recalling the problem (10). In this case, only one feasible solution of  $\mathbf{W}_B^{up} = \frac{P_B}{\|\mathbf{h}_{IR}\|^2} \mathbf{h}_{IR} \mathbf{h}_{IR}^H$  exists for the problem (13), so it is also globally optimal. Meanwhile, the non-negative dual variables  $\lambda^*$  and  $\beta^*$  corresponding to constraints  $\widetilde{\text{CR1}}$  and  $\widetilde{\text{CR2}}$  can be set randomly since they are irrelevant to  $\mathbf{W}_B^{up}$ . For the following analysis, we adopt  $\lambda^* = 0$  and  $\beta^* = +\infty$  when  $R_I = R_I^{up}$ . In the sequel, we mainly consider the case of  $0 \leq R_I < R_I^{up}$  in which the problem (13) is strictly feasible and semi-closed optimal solutions of  $\{\mathbf{W}_B^*, \mathbf{P}_{E_k}^*, \forall k\}$  can be found. Based on the definitions  $\widetilde{\mathbf{W}}_B^* = \tau_0 \mathbf{W}_B^*$ ,  $\mathbf{P}_{E_k}^* = (1 - \tau_0) \mathbf{P}_{E_k}^*$ ,  $\forall k \in \mathcal{K}$  and the Lagrangian function in (14), the Karush-Kuhn-Tucker (KKT) conditions of the problem (13) w.r.t.  $\mathbf{W}_B^*$  and  $\mathbf{P}_{E_k}^*$  can be written as

$$\widetilde{\mathbf{H}}^* + \mathbf{Z}_0^* = \mathbf{0}_{N_B}, \mathbf{Z}_0^* \mathbf{W}_B^* = \mathbf{0}, \mathbf{Z}_0^* \succeq \mathbf{0}, \quad (24a)$$

$$\mathbf{G}_{E_k}^H \mathbf{M}_{\mathcal{K} \setminus k}^{*\frac{1}{2}} (\mathbf{I}_{N_B} + \sigma_n^{-2} \mathbf{M}_{\mathcal{K} \setminus k}^{*\frac{1}{2}} \mathbf{G}_{E_k} \mathbf{P}_{E_k}^* \mathbf{G}_{E_k}^H \mathbf{M}_{\mathcal{K} \setminus k}^{*\frac{1}{2}})^{-1} \\ \times \mathbf{M}_{\mathcal{K} \setminus k}^{*\frac{1}{2}} \mathbf{G}_{E_k} = \sigma_n^2 \ln 2 (\mu_k^* \mathbf{I}_{N_U} - \mathbf{Z}_k^*), \quad (24b)$$

$$\mathbf{Z}_k \mathbf{P}_{E_k}^* = \mathbf{0}, \mathbf{Z}_k^* \succeq \mathbf{0}, \forall k \quad (24c)$$

$$\lambda^* (\text{tr}(\mathbf{W}_B^*) - P_B) = 0, \quad (24d)$$

$$\beta^* (\text{tr}(\mathbf{h}_{IR}^H \mathbf{W}_B^* \mathbf{h}_{IR}) - \sigma_n^2 (2^{\frac{R_I}{\tau_0}} - 1)) = 0, \quad (24e)$$

$$\mu_k^* ((1 - \tau_0) \text{tr}(\mathbf{P}_{E_k}^*) - \tau_0 \varepsilon_k \text{tr}(\mathbf{H}_{E_k} \mathbf{W}_B^* \mathbf{H}_{E_k}^H)) = 0, \forall k, \quad (24f)$$

The optimal solutions of  $\{\mathbf{W}_B^*, \lambda^*, \beta^*\}$  and  $\{\mathbf{P}_{E_k}^*, \forall k, \mu_k^*\}$  can then be derived individually based on above KKT conditions as follows.

##### A. The optimal $\mathbf{W}_B^*$ , $\lambda^*$ and $\beta^*$

Recalling that  $\widetilde{\mathbf{H}}^* = \mathbf{H}^* - \lambda^* \mathbf{I}_{N_B}$  in (15), we firstly define the eigenvalue decomposition (EVD)  $\mathbf{H}^* = \mathbf{U}_H \mathbf{\Lambda}_H \mathbf{U}_H^H$ , where the maximum eigenvalue  $\lambda_{H, \max}$  in the diagonal matrix  $\mathbf{\Lambda}_H$  satisfies  $\lambda_{H, \max} > 0$  since  $\mathbf{H}^* \succeq \mathbf{0}$  according to its definition in (15). Then  $\widetilde{\mathbf{H}}^*$  can be rewritten as  $\widetilde{\mathbf{H}}^* = \mathbf{U}_H (\mathbf{\Lambda}_H - \lambda^* \mathbf{I}_{N_B}) \mathbf{U}_H^H$ . Further based on the KKT condition (24a), we simultaneously have  $\widetilde{\mathbf{H}}^* = -\mathbf{Z}_0^* \preceq \mathbf{0}$  and  $\widetilde{\mathbf{H}}^* \mathbf{W}_B^* = \mathbf{0}$ . Therefore,  $\widetilde{\mathbf{H}}^*$  must be singular and thus the optimal  $\lambda^*$  satisfies  $\lambda^* = \lambda_{H, \max} > 0$ .

Moreover, we have  $\mathbf{W}_B^* = c \mathbf{u}_H \mathbf{u}_H^H$ , where  $\mathbf{u}_H$  is the unit-norm eigenvector of  $\mathbf{H}^*$  corresponding to  $\lambda_{H, \max}$ . and  $c$  is a constant. Meanwhile, according to the KKT condition (24d), we have  $\text{tr}(\mathbf{W}_B^*) = P_B$  due to  $\lambda^* > 0$ , so the constant  $c = P_B$  is derived. As a result, the optimal  $\mathbf{W}_B^*$  and  $\lambda^*$  are finally given as (16a) in Theorem 1, i.e.,

$$(\mathbf{W}_B^*, \lambda^*) = \begin{cases} (P_B \mathbf{u}_H \mathbf{u}_H^H, \lambda_{H, \max}^*) & 0 \leq R_I < R_I^{up} \\ (\frac{P_B}{\|\mathbf{h}_{IR}\|^2} \mathbf{h}_{IR} \mathbf{h}_{IR}^H, 0) & R_I = R_I^{up} \end{cases} \quad (25)$$

As for the optimal  $\beta^*$ , we firstly observe that when  $0 \leq R_I < R_I^{mi}$ , as discussed in Section III. B, the downlink rate constraint is inactive, i.e.,  $f_R(\mathbf{W}_B^*) = \tau_0 \log(1 + \sigma_n^{-2} \mathbf{h}_{IR}^H \mathbf{W}_B^* \mathbf{h}_{IR}) > R_I$ . It is equivalent to  $\text{tr}(\mathbf{h}_{IR}^H \mathbf{W}_B^* \mathbf{h}_{IR}) > \sigma_n^2 (2^{\frac{R_I}{\tau_0}} - 1)$ . Based on the KKT condition (24e), it directly yields that  $\beta^* = 0$  when  $0 \leq R_I < R_I^{mi}$ . On the other hand, when  $R_I^{mi} < R_I < R_I^{up}$ , recalling Lemma 1, the downlink rate constraint is tight, i.e.,  $f_R(\mathbf{W}_B^*) = \tau_0 \log(1 + \sigma_n^{-2} \mathbf{h}_{IR}^H \mathbf{W}_B^* \mathbf{h}_{IR}) = R_I$ . Thus the optimal  $\beta^*$  which affects the optimal  $\mathbf{W}_B^*$  implicitly through  $\mathbf{H}^*$  should satisfy the nonlinear equation  $f_R(\mathbf{W}_B^*) = R_I$ . As shown in Appendix A,  $R_I^{mi}$  is a critical point at which the inactive downlink rate constraint becomes tight, so we can still adopt  $\beta^* = 0$  for  $R_I = R_I^{mi}$ . Now combining the above results with that for the special case of  $R_I = R_I^{up}$  discussed in the beginning, we can summarize the optimal  $\beta^*$  as

$$\beta^* = \begin{cases} 0 & 0 \leq R_I \leq R_I^{mi} \\ \arg \{f_R(\mathbf{W}_B^*) = R_I\} & R_I^{mi} < R_I < R_I^{up} \\ +\infty & R_I = R_I^{up} \end{cases}, \quad (26)$$

as shown in (16f).

##### B. The optimal $\mathbf{P}_{E_k}^*$ and $\mu_k^*$ , $\forall k$

To derive the optimal  $\mathbf{P}_{E_k}^*$ ,  $\forall k$ , all related KKT conditions (24b), (24c) and (24f) should be jointly considered. It is noted that these KKT conditions are with the same structure as that of the conventional MIMO rate maximization problem subject to the total transmit power constraint, as shown in [25]. Therefore, the optimal structure of  $\mathbf{P}_{E_k}^*$ ,  $\forall k$  derived in [25] is also applicable to our problem. Specifically, based on the SVD  $\mathbf{M}_{\mathcal{K} \setminus k}^{*\frac{1}{2}} \mathbf{G}_{E_k} = \mathbf{U}_{M_{\mathcal{K} \setminus k}}^* \mathbf{\Lambda}_{M_{\mathcal{K} \setminus k}}^* \mathbf{V}_{M_{\mathcal{K} \setminus k}}^{*H}$ ,  $\forall k$ , the optimal  $\mathbf{P}_{E_k}^*$  is given by  $\mathbf{P}_{E_k}^* = \mathbf{V}_{M_{\mathcal{K} \setminus k}}^* \mathbf{\Lambda}_{P_{E_k}}^* \mathbf{V}_{M_{\mathcal{K} \setminus k}}^{*H}$ ,  $\forall k$ , where the diagonal matrix  $\mathbf{\Lambda}_{P_{E_k}}^* = \text{diag}[\Lambda_{P_{E_k}, 1}^*, \dots, \Lambda_{P_{E_k}, N_U}^*]$  needs to be optimized. Further based on (24b) and (24c), we have

$$(\sigma_n^2 \ln 2 \mu_k^* \mathbf{I}_{N_U} - \mathbf{G}_{E_k}^H \mathbf{M}_{\mathcal{K} \setminus k}^{*\frac{1}{2}} (\mathbf{I}_{N_B} + \sigma_n^{-2} \mathbf{M}_{\mathcal{K} \setminus k}^{*\frac{1}{2}} \mathbf{G}_{E_k} \mathbf{P}_{E_k}^* \mathbf{G}_{E_k}^H \mathbf{M}_{\mathcal{K} \setminus k}^{*\frac{1}{2}})^{-1} \mathbf{M}_{\mathcal{K} \setminus k}^{*\frac{1}{2}} \mathbf{G}_{E_k}) \mathbf{P}_{E_k}^* = \mathbf{0} \quad (27)$$

Then by substituting the analytical structure of  $\mathbf{P}_{E_k}^*$  into (27), the optimal  $\Lambda_{P_{E_k}, i}^*$  can be derived as (16d), i.e.,

$$\Lambda_{P_{E_k}, i}^* = \left[ \frac{1}{\ln 2 \mu_k^*} - \frac{\sigma_n^2}{\Lambda_{M_{\mathcal{K} \setminus k}, i}^{*2}} \right]^+, \quad \forall i, \forall k. \quad (28)$$

Next, to obtain the optimal  $\mu_k^*, \forall k$ , we firstly prove  $\mu_k^* > 0, \forall k$  for the problem (13). Specifically, based on (24b) and (24c), we have

$$\begin{aligned} \sigma_n^2 \ln 2 \mathbf{Z}_k^* &= \sigma_n^2 \ln 2 \mu_k^* \mathbf{I}_{N_U} - \mathbf{G}_{E_k}^H \mathbf{M}_{\mathcal{K} \setminus k}^{\star \frac{1}{2}} (\mathbf{I}_{N_B} \\ &\quad + \sigma_n^{-2} \mathbf{M}_{\mathcal{K} \setminus k}^{\star \frac{1}{2}} \mathbf{G}_{E_k} \mathbf{P}_{E_k}^* \mathbf{G}_{E_k}^H \mathbf{M}_{\mathcal{K} \setminus k}^{\star \frac{1}{2}})^{-1} \mathbf{M}_{\mathcal{K} \setminus k}^{\star \frac{1}{2}} \mathbf{G}_{E_k} \\ &\preceq \sigma_n^2 \ln 2 \mu_k^* \mathbf{I}_{N_U} \end{aligned} \quad (29)$$

It is clear that  $\mu_k^* > 0, \forall k$  must hold since  $\mathbf{Z}_k^* \succeq \mathbf{0}$ . Then based on the KKT condition (24f), we have  $(1 - \tau_0) \text{tr}(\mathbf{P}_{E_k}^*) = (1 - \tau_0) \text{tr}(\mathbf{\Lambda}_{P_{E_k}}) = \tau_0 \varepsilon_k \text{tr}(\mathbf{H}_{E_k} \mathbf{W}_B^* \mathbf{H}_{E_k}^H)$ . By substituting (28) into this equation, the optimal  $\mu_k^* = \frac{N_U(1-\tau_0)}{\ln 2 \left( \tau_0 \varepsilon_k \text{tr}(\mathbf{H}_{E_k} \mathbf{W}_B^* \mathbf{H}_{E_k}^H) + \sum_{i=1}^{N_U} \frac{(1-\tau_0) \sigma_n^2}{\lambda_{M_{\mathcal{K} \setminus k}^*, i}^2} \right)}$ ,  $\forall k$ , is obtained as (16e), which finally completes the proof.

## APPENDIX C

Based on the analysis in Section III. A, it is easy to obtain that the achievable downlink rate function  $f_R(\mathbf{W}_B)$  is bounded as  $0 \leq f_R(\mathbf{W}_B) \leq R_I^{up}$ . Now given a downlink rate threshold  $R_I$  with  $R_I^{mi} < R_I < R_I^{up}$ , we firstly consider  $\beta=0$  and prove  $f_R(\mathbf{W}_B)|_{\beta=0} < R_I$  by contradiction as follows. If  $f_R(\mathbf{W}_B)|_{\beta=0} \geq R_I$  holds, we readily observe that the optimal  $\mathbf{W}_B^*$  is only determined by the ERs downlink channels in the form of (16a), and actually not influenced by the downlink rate constraint. However, as analyzed in Section III. B, this case only happens when the downlink threshold  $R_I$  is no more than  $R_I^{mi}$ , i.e.,  $R_I \leq R_I^{mi}$ , which clearly contradicts with the original assumption of  $R_I^{mi} < R_I < R_I^{up}$ . Thus it proves that  $f_R(\mathbf{W}_B)|_{\beta=0} < R_I$ . On the other hand, when  $\beta \rightarrow +\infty$ , we have  $\frac{\mathbf{H}^*}{\beta} \rightarrow \sigma_n^{-2} \mathbf{h}_{I_R} \mathbf{h}_{I_R}^H$  and  $\mathbf{u}_H \rightarrow \frac{\mathbf{h}_{I_R}}{\|\mathbf{h}_{I_R}\|}$  from Theorem 1. Together with the bounded property of  $f_R(\mathbf{W}_B)$ , it follows that  $f_R(\mathbf{W}_B)|_{\beta=+\infty} = R_I^{up}$ . Then we can naturally conclude that  $0 \leq f_R(\mathbf{W}_B)|_{\beta=0} < R_I < f_R(\mathbf{W}_B)|_{\beta=+\infty} = R_I^{up}$ .

Next, given  $R_I^{mi} < R_I < R_I^{up}$ , we prove that there exists a unique  $\beta^* \in (0, \infty)$  satisfying  $f_R(\mathbf{W}_B^*) = R_I$  by contradiction as follows. Since the problem (13) is strictly concave, there exists one unique and globally optimal  $\mathbf{W}_B^*$ . Assuming that there are two  $\beta_1$  and  $\beta_2$  ( $\beta_1 < \beta_2$ ) simultaneously realizing the optimal  $\mathbf{W}_B^*$ , and denoting the corresponding composite matrices  $\mathbf{H}^* \succeq \mathbf{0}$  in Theorem 1 as  $\mathbf{H}_1^* \succeq \mathbf{0}$  and  $\mathbf{H}_2^* \succeq \mathbf{0}$ , respectively, then we readily have

$$\mathbf{H}_1^* = \mathbf{H}_2^* + \mathbf{H}_{I_R}, \quad \mathbf{H}_{I_R} = (\beta_2 - \beta_1) \mathbf{h}_{I_R} \mathbf{h}_{I_R}^H. \quad (30)$$

Recalling (16a), it is clear that for obtaining the unique  $\mathbf{W}_B^* = P_B \mathbf{u}_H \mathbf{u}_H^H$ , the dominant eigenspaces of  $\mathbf{H}_1^*$  and  $\mathbf{H}_2^*$  should be identical. Therefore, we can define the EVDs  $\mathbf{H}_i^* = \mathbf{U}_{H_i} \mathbf{\Lambda}_{H_i} \mathbf{U}_{H_i}^H$ , where the unitary matrix is  $\mathbf{U}_{H_i} = [\mathbf{u}_H, \tilde{\mathbf{U}}_{H_i}]$  and the diagonal matrix is  $\mathbf{\Lambda}_{H_i} = \text{diag}[\lambda_{H_i, \max}, \lambda_{H_i, 2}, \dots, \lambda_{H_i, N_B}] \succeq \mathbf{0}$ . Based on  $\mathbf{u}_H^H \tilde{\mathbf{U}}_{H_1} = \mathbf{0}$  and  $\mathbf{u}_H^H \tilde{\mathbf{U}}_{H_2} = \mathbf{0}$ , we have  $\tilde{\mathbf{U}}_{H_1} = \tilde{\mathbf{U}}_{H_2} \mathbf{Q}$ , where  $\mathbf{Q} \in \mathbb{C}^{(N_B-1) \times (N_B-1)}$  is an arbitrary unitary matrix. Further by

defining  $\tilde{\mathbf{\Lambda}}_{H_i} = \text{diag}[\lambda_{H_i, 2}, \dots, \lambda_{H_i, N_B}]$ ,  $i = 1, 2$ , the equation (30) can be rewritten as

$$\begin{aligned} \mathbf{H}_{I_R} &= \mathbf{H}_1^* - \mathbf{H}_2^* \\ &= \underbrace{(\lambda_{H_1, \max} - \lambda_{H_2, \max})}_{\Delta \lambda} \mathbf{u}_H \mathbf{u}_H^H + \underbrace{\tilde{\mathbf{U}}_{H_2} (\mathbf{Q} \tilde{\mathbf{\Lambda}}_{H_1} \mathbf{Q}^H - \tilde{\mathbf{\Lambda}}_{H_2}) \tilde{\mathbf{U}}_{H_2}^H}_{\tilde{\mathbf{Q}}_H} \end{aligned} \quad (31)$$

Since  $\mathbf{u}_H^H \tilde{\mathbf{U}}_{H_2} = \mathbf{0}$  denoting the orthogonal space, to guarantee the rank-1 positive semidefinite  $\mathbf{H}_{I_R}$ , only the following two cases are possible:

1) *case1*:  $\Delta \lambda \neq 0$  and  $\tilde{\mathbf{U}}_{H_2} \tilde{\mathbf{Q}}_H^{\frac{1}{2}} = \mathbf{0}$ : In this case, we readily have  $\mathbf{H}_{I_R} = \Delta \lambda \mathbf{u}_H \mathbf{u}_H^H$  from (31) and thus the optimal downlink beamforming  $\mathbf{W}_B^* = P_B \mathbf{u}_H \mathbf{u}_H^H = P_B \mathbf{h}_{I_R} \mathbf{h}_{I_R}^H / \|\mathbf{h}_{I_R}\|^2$  is derived, which implies that  $f_R(\mathbf{W}_B^*) = R_I^{up} > R_I$ .

2) *case2*:  $\Delta \lambda = 0$  and  $\text{rank}(\tilde{\mathbf{U}}_{H_2} \tilde{\mathbf{Q}}_H^{\frac{1}{2}}) = 1$ : In this case,  $\mathbf{H}_{I_R} = \tilde{\mathbf{U}}_{H_2} (\mathbf{Q} \tilde{\mathbf{\Lambda}}_{H_1} \mathbf{Q}^H - \tilde{\mathbf{\Lambda}}_{H_2}) \tilde{\mathbf{U}}_{H_2}^H$  is observed from (31) and thus we have  $\mathbf{u}_H^H \mathbf{H}_{I_R} \mathbf{u}_H = 0$ , which implies that  $f_R(\mathbf{W}_B^*) = 0 < R_I$ .

It is obvious that both the two cases contradict with the original equation of  $f_R(\mathbf{W}_B^*) = R_I$ . As a result, we conclude that there is only one optimal  $\beta^* \in (0, \infty)$  satisfying  $f_R(\mathbf{W}_B^*) = R_I$ . Meanwhile,  $f_R(\mathbf{W}_B)$  is also continuous due to the EVD operation on positive semidefinite matrices and log function. Overall, when  $R_I^{mi} < R_I < R_I^{up}$ , with the boundness, uniqueness and continuity of  $f_R(\mathbf{W}_B)$ , we easily conclude that  $f_R(\mathbf{W}_B)$  is monotonic w.r.t.  $\beta \in (0, \infty)$ . Moreover, since  $f_R(\mathbf{W}_B)|_{\beta=0} < f_R(\mathbf{W}_B)|_{\beta=+\infty}$ , we can infer that  $f_R(\mathbf{W}_B)$  is monotonically increasing w.r.t.  $\beta \in (0, \infty)$  and converges to  $R_I^{up}$ . This completes the proof.

## APPENDIX D

For the problem (17), the KKT conditions are given by

$$(24a), (24d), (24e) \quad (32a)$$

$$\frac{\sigma_n^{-2}}{\ln 2} \mathbf{G}_{E_k}^H (\mathbf{I}_{N_B} + \frac{\sigma_n^{-2}}{\tau_{E_k}} \mathbf{G}_{E_k} \tilde{\mathbf{P}}_{E_k}^* \mathbf{G}_{E_k}^H)^{-1} \mathbf{G}_{E_k} = \mu_k^* \mathbf{I}_{N_U} - \mathbf{Z}_k^*, \quad (32b)$$

$$\mathbf{Z}_k^* \tilde{\mathbf{P}}_{E_k}^* = \mathbf{0}, \quad \mathbf{Z}_k^* \succeq \mathbf{0}, \quad \forall k \quad (32c)$$

$$\mu_k^* (\text{tr}(\tilde{\mathbf{P}}_{E_k}^*) - \tau_0 \varepsilon_k \text{tr}(\mathbf{H}_{E_k} \mathbf{W}_B^* \mathbf{H}_{E_k}^H)) = 0, \quad \forall k \quad (32d)$$

$$\begin{aligned} \log \det(\mathbf{I}_{N_B} + \frac{\sigma_n^{-2}}{\tau_{E_k}^*} \mathbf{G}_{E_k} \tilde{\mathbf{P}}_{E_k}^* \mathbf{G}_{E_k}^H) - \frac{\sigma_n^{-2}}{\ln 2 \tau_{E_k}^*} \text{tr}((\mathbf{I}_{N_B} \\ + \frac{\sigma_n^{-2}}{\tau_{E_k}^*} \mathbf{G}_{E_k} \tilde{\mathbf{P}}_{E_k}^* \mathbf{G}_{E_k}^H)^{-1} \mathbf{G}_{E_k} \tilde{\mathbf{P}}_{E_k}^* \mathbf{G}_{E_k}^H) = 0 \end{aligned} \quad (32e)$$

$$\tau_{I_R}^* (C_R - \gamma^*) = 0, \quad \forall k, \quad \tau_{I_R}^* + \sum_{k=1}^K \tau_{E_k}^* = 1 - \tau_0. \quad (32f)$$

### A. The optimal $\mathbf{W}_B^*$ , $\lambda^*$ and $\beta^*$

Since the TDMA-enabled WPSNs have the same downlink transmission as the SDMA-enabled WPCNs, it is clear that the  $\{\mathbf{W}_B^*, \lambda^*, \beta^*\}$ -related KKT conditions of the problem (17) are exactly the same as that for the problem (13), i.e., (24a), (24d), and (24e). So following the same approach in Appendix B. A, we can derive the same optimal  $\mathbf{W}_B^*$  and  $\lambda^*, \beta^*$  as in (25) and (26), respectively, to the problem (17).

### B. The optimal $\mathbf{P}_{E_k}^*$ and $\mu_k^*, \forall k$

The  $\{\mathbf{P}_{E_k}^*, \mu_k^*\}$ -related KKT conditions ((32b),(32c)), (32d) are similar to that of the MIMO capacity maximization in [25]. Therefore, the optimal  $\tilde{\mathbf{P}}_{E_k}^*, \forall k$  can be derived as  $\tilde{\mathbf{P}}_{E_k}^* = \mathbf{V}_{G_{E_k}} \mathbf{\Lambda}_{P_{E_k}} \mathbf{V}_{G_{E_k}}^H, \forall k$ , where  $\mathbf{V}_{G_{E_k}}$  comes from the SVD  $\mathbf{G}_{E_k} = \mathbf{U}_{G_{E_k}} \mathbf{\Lambda}_{G_{E_k}} \mathbf{V}_{G_{E_k}}^H$  and the positive diagonal  $\mathbf{\Lambda}_{P_{E_k}} = \text{diag}[\Lambda_{P_{E_k},1}, \dots, \Lambda_{P_{E_k},N_U}]$  needs to be determined. Similarly to that in Appendix B. B, we can obtain  $\Lambda_{P_{E_k},i} = [\frac{\tau_{E_k}^*}{\ln 2\mu_k^*} - \frac{\sigma_n^2 \tau_{E_k}^*}{\Lambda_{G_{E_k},i}^2}]^+, \forall i$ , by substituting the analytical structure of  $\tilde{\mathbf{P}}_{E_k}^*, \forall k$  into the KKT conditions (32b) and (32c). Further based on  $\tilde{\mathbf{P}}_{E_k}^* = \tau_{E_k}^* \mathbf{P}_{E_k}^*, \forall k$ , we readily have the optimal  $\mathbf{P}_{E_k}^* = \mathbf{V}_{G_{E_k}} \mathbf{\Lambda}_{P_{E_k}} \mathbf{V}_{G_{E_k}}^H / \tau_{E_k}^*$  as (19a) in Theorem 2. Moreover, we also have  $\mu_k^* > 0, \forall k$  for the problem (17) by jointly considering (32b),  $\mathbf{Z}_k^* \succeq \mathbf{0}$  and  $\mathbf{G}_{E_k}^H (\mathbf{I}_{N_B} + \frac{\sigma_n^2}{\tau_{E_k}^*} \mathbf{G}_{E_k} \tilde{\mathbf{P}}_{E_k}^* \mathbf{G}_{E_k}^H)^{-1} \mathbf{G}_{E_k} \succeq \mathbf{0}$ . Then based on the KKT condition (32d),  $\text{tr}(\tilde{\mathbf{P}}_{E_k}^*) = \text{tr}(\mathbf{\Lambda}_{P_{E_k}}) = \tau_0 \varepsilon_k \text{tr}(\mathbf{H}_{E_k} \mathbf{W}_B^* \mathbf{H}_{E_k}^H)$  holds. Hence, the optimal  $\mu_k^* = \frac{N_U \tau_{E_k}^*}{\ln 2 \left( \tau_0 \varepsilon_k \text{tr}(\mathbf{H}_{E_k} \mathbf{W}_B^* \mathbf{H}_{E_k}^H) + \sum_{i=1}^{N_U} \frac{\sigma_n^2 \tau_{E_k}^*}{\Lambda_{G_{E_k},i}^2} \right)}, \forall k$ , is derived as (19d).

### C. The optimal $\tau_{up}^*$ and $\gamma^*$

By substituting the above analytical structure of  $\tilde{\mathbf{P}}_{E_k}^*$  into the  $\{\tau_{E_k}^*, \forall k\}$ -related KKT condition (32e), we have

$$g_T(\tau_{E_k}^*) = \sum_{i=1}^{N_U} \left( \log \left( 1 + \frac{\sigma_n^2 \bar{\Lambda}_{G_{E_k},i}}{\tau_{E_k}^*} \right) - \frac{\sigma_n^2 \bar{\Lambda}_{G_{E_k},i}}{\ln 2 (\tau_{E_k}^* + \sigma_n^2 \bar{\Lambda}_{G_{E_k},i})} \right) = \gamma^*, \forall k \quad (33)$$

where  $\bar{\Lambda}_{G_{E_k},i} = \Lambda_{G_{E_k},i}^2 \Lambda_{P_{E_k},i}, \forall i$ . Since the problem (17) is strictly concave, the Lagrangian function in (18) should be upper bounded for the optimization variables  $\{\tau_{up}, \tilde{\mathbf{W}}_B, \tilde{\mathbf{P}}_{E_k}, \forall k\}$  in  $\mathcal{A}_T$ . Now with respect to the non-negative variable  $\tau_{IR}$ , the corresponding term in (18) should be upper bounded, which implies that  $C_R - \gamma^* \leq 0$ . Then together with (33) and the KKT condition (32f), only the following two cases are possible for deriving the optimal  $\tau_{up}^*$  and  $\gamma^*$ .

1) *case1*:  $C_R - \gamma^* < 0$ : It directly follows from the KKT condition (32f) that  $\tau_{IR}^* = 0$  and  $\sum_{k=1}^K \tau_{E_k}^* = 1 - \tau_0$ . Then the optimal  $\tau_{E_k}^* = (\tau_{E_k})^+, \forall k$  and  $\gamma^*$  can be jointly derived from the equations  $g_T(\tau_{E_k}) = \gamma^*, \forall k$  and  $\sum_{k=1}^K (\tau_{E_k})^+ = 1 - \tau_0$ , as shown in (19e) for the case of  $\gamma^* > C_R$ .

2) *case2*:  $C_R - \gamma^* = 0$ : In this case, we have  $\gamma^* = C_R$ . Then referring to (33), the optimal  $\tau_{E_k}^* = (\tau_{E_k})^+, \forall k$  can be obtained from  $g_T(\tau_{E_k}) = C_R, \forall k$ . Moreover, the optimal timing allocation for the IR is determined as  $\tau_{IR}^* = (\tau_{IR})^+$  and  $\tau_{IR} = 1 - \tau_0 - \sum_{k=1}^K (\tau_{E_k})^+$ , which finally completes the proof.

### REFERENCES

[1] A. Al Fugaha, M. Guizani, et. al., "Internet of Things: a survey on enabling technologies, protocols, and applications," *IEEE Commun. Surveys Tut.*, vol. 17, no. 4, pp. 2347–2376, Jun. 2015.

[2] J. Santos, J. J. P. C. Rodrigues, et. al., "Intelligent personal assistants based on Internet of Things approaches," *IEEE Syst. J.*, pp. 1–10, 2016.

[3] P. Ramezani and A. Jamalipour, "Toward the evolution of wireless powered communication networks for the future Internet of Things," *IEEE Network*, vol. 31, no. 6, pp. 62–69, Dec. 2017.

[4] J. Liu, K. Xiong, P. Fan and Z. Zhong, "Resource allocation in wireless powered sensor networks with circuit energy consumption constraints," *IEEE Access*, vol. 5, pp. 22775–22782, 2017.

[5] K. W. Choi, P. A. Rosyady, L. Ginting, A. A. Aziz, D. Setiawan and D. I. Kim, "Theory and experiment for wireless-powered sensor networks: how to keep sensors alive," *IEEE Trans. Wireless Commun.*, vol. 17, no. 1, pp. 430–444, Jan. 2018.

[6] K. W. Choi, L. Ginting, P. A. Rosyady, A. A. Aziz and D. I. Kim, "Wireless-powered sensor networks: how to realize," *IEEE Trans. Wireless Commun.*, vol. 16, no. 1, pp. 221–234, Jan. 2017.

[7] Z. Chu, F. Zhou, Z. Zhu, R. Q. Hu and P. Xiao, "Wireless powered sensor networks for Internet of Things: maximum throughput and optimal power allocation," *IEEE Internet Things*, vol. 5, no. 1, pp. 310–321, Feb. 2018.

[8] M. Song and M. Zheng, "Energy efficiency optimization for wireless powered sensor networks with nonorthogonal multiple access," *IEEE Sensors Lett.*, vol. 2, no. 1, pp. 1–4, Mar. 2018.

[9] A. M. Zungeru, L. M. Ang, S. Prabaharan, and K. P. Seng, "Radio frequency energy harvesting and management for wireless sensor networks," in *Green Mobile Devices and Networks*, FL, USA: CRC Press, 2012, pp. 341–368.

[10] S. He et al., "Energy provisioning in wireless rechargeable sensor networks," *IEEE Trans. Mobile Comput.*, vol. 12, no. 10, pp. 1931–1942, Oct. 2013.

[11] X. Lu, P. Wang, D. Niyato, D. I. Kim and Z. Han, "Wireless charging technologies: fundamentals, standards, and network applications," *IEEE Commun. Surveys Tuts.*, vol. 18, no. 2, pp. 1413–1452, Nov. 2015.

[12] R. Zhang and C. K. Ho, "MIMO broadcasting for simultaneous wireless information and power transfer," *IEEE Trans. Wireless Commun.*, vol. 12, no. 5, pp. 1989–2001, May 2013.

[13] S. Bi, Y. Zeng and R. Zhang, "Wireless powered communication networks: an overview," *IEEE Wireless Commun.*, vol. 23, no. 2, pp. 10–18, Apr. 2016.

[14] H. Ju and R. Zhang, "Optimal resource allocation in full-duplex wireless-powered communication network," *IEEE Trans. Commun.*, vol. 62, no. 10, pp. 3528–3540, Oct. 2014.

[15] S. Lee and R. Zhang, "Cognitive wireless powered network: spectrum sharing models and throughput maximization," *IEEE Trans. Cognitive Commun. and Net.*, vol. 1, no. 3, pp. 335–346, Sept. 2015.

[16] L. Liu, R. Zhang, and K. C. Chua, "Multi-antenna wireless powered communication with energy beamforming," *IEEE Trans. Commun.*, vol. 62, no. 12, pp. 4349–4361, Dec. 2014.

[17] J. Kim, H. Lee, C. Song, T. Oh and I. Lee, "Sum throughput maximization for multi-user MIMO cognitive wireless powered communication networks," *IEEE Trans. Wireless Commun.*, vol. 16, no. 2, pp. 913–923, Feb. 2017.

[18] G. Yang, C. K. Ho, R. Zhang, and Y. L. Guan, "Throughput optimization for massive MIMO systems powered by wireless energy transfer," *IEEE J. Sel. Areas Commun.*, vol. 33, no. 8, pp. 1640–1650, Aug. 2015.

[19] H. Ju and R. Zhang, "Throughput maximization in wireless powered communication networks," *IEEE Trans. Wireless Commun.*, vol. 13, no. 1, pp. 418–428, Jan. 2014.

[20] Y. L. Che, L. Duan, and R. Zhang, "Spatial throughput maximization of wireless powered communication networks," *IEEE J. Sel. Areas Commun.*, vol. 33, no. 8, pp. 1534–1548, Aug. 2015.

[21] Q. Sun, G. Zhu, C. Shen, X. Li and Z. Zhong, "Joint beamforming design and time allocation for wireless powered communication networks," *IEEE Commun. Lett.*, vol. 18, no. 10, pp. 1783–1786, Oct. 2014.

[22] Y. Gao, W. Cheng, H. Zhang and Z. Li, "Optimal resource allocation with heterogeneous QoS provisioning for wireless powered sensor networks," in *Proc. IEEE GLOBECOM*, Singapore, 2017, pp. 1–6.

[23] M. U. Kim and H. J. Yang, "Min-SINR maximization with DL SWIPT and UL WPSN in multi-antenna interference networks," *IEEE Wireless Commun. Lett.*, vol. 6, no. 3, pp. 318–321, Jun. 2017.

[24] L. Zhou and W. Yu, "Uplink multicell processing with limited backhaul via per-base-station successive interference cancellation," *IEEE J. Sel. Areas Commun.*, vol. 31, no. 10, pp. 1981–1993, Oct. 2013.

[25] R. Zhang, Y. C. Liang, and S. Cui, "Dynamic resource allocation in cognitive radio networks," *IEEE Signal Process. Mag.*, vol. 27, no. 3, pp. 102–114, May 2010.

[26] S. Boyd and L. Vandenberghe, *Convex Optimization*. Cambridge, U.K.: Cambridge Univ. Press, 2004.

- [27] W. Yu, W. Rhee, S. Boyd, and J. M. Cioffi, "Iterative water-filling for Gaussian vector multiple-access channels," *IEEE Trans. Inf. Theory*, vol. 50, no. 1, pp. 145–152, Jan. 2004.
- [28] V. Nguyen, H. D. Tuan, H. H. Nguyen and N. N. Tran, "Optimal superimposed training design for spatially correlated fading MIMO channels," *IEEE Trans. Wireless Commun.*, vol. 7, no. 8, pp. 3206–3217, Aug. 2008.
- [29] J. Kiefer, "Sequential minimax search for a maximum," in *Proc. Amer. Math. Soc.*, vol. 4, no. 3, pp. 502–506, 1953.
- [30] A. Ben-Tal and A. Nemirovski, "Lectures on modern convex optimization: analysis, algorithms, and engineering applications," *ser. MPSIAM series on optimization*, Philadelphia, PA, USA: SIAM, 2001.